Atmospheric
Chemistry
and Physics

Open Access

Black carbon in the Arctic: the underestimated role of gas flaring and residential combustion emissions

A. Stohl[1], Z. Klimont[2], S. Eckhardt[1], K. Kupiainen[2,3], V. P. Shevchenko[4], V. M. Kopeikin[5], and A. N. Novigatsky[4]

[1]NILU – Norwegian Institute for Air Research, Kjeller, Norway
[2]International Institute for Applied Systems Analysis (IIASA), Laxenburg, Austria
[3]Finnish Environment Institute (SYKE), Helsinki, Finland
[4]P.P. Shirshov Institute of Oceanology, Russian Academy of Sciences, Moscow, Russia
[5]A.M. Obukhov Institute of Atmospheric Physics, Russian Academy of Sciences, Moscow, Russia

Correspondence to: A. Stohl (ast@nilu.no)

Abstract. Arctic haze is a seasonal phenomenon with high concentrations of accumulation-mode aerosols occurring in the Arctic in winter and early spring. Chemistry transport models and climate chemistry models struggle to reproduce this phenomenon, and this has recently prompted changes in aerosol removal schemes to remedy the modeling problems. In this paper, we show that shortcomings in current emission data sets are at least as important. We perform a 3 yr model simulation of black carbon (BC) with the Lagrangian particle dispersion model FLEXPART. The model is driven with a new emission data set ("ECLIPSE emissions") which includes emissions from gas flaring. While gas flaring is estimated to contribute less than 3 % of global BC emissions in this data set, flaring dominates the estimated BC emissions in the Arctic (north of 66° N). Putting these emissions into our model, we find that flaring contributes 42 % to the annual mean BC surface concentrations in the Arctic. In March, flaring even accounts for 52 % of all Arctic BC near the surface. Most of the flaring BC remains close to the surface in the Arctic, so that the flaring contribution to BC in the middle and upper troposphere is small. Another important factor determining simulated BC concentrations is the seasonal variation of BC emissions from residential combustion (often also called domestic combustion, which is used synonymously in this paper). We have calculated daily residential combustion emissions using the heating degree day (HDD) concept based on ambient air temperature and compare results from model simulations using emissions with daily, monthly and annual time resolution. In January, the Arctic-mean surface concen-

trations of BC due to residential combustion emissions are 150 % higher when using daily emissions than when using annually constant emissions. While there are concentration reductions in summer, they are smaller than the winter increases, leading to a systematic increase of annual mean Arctic BC surface concentrations due to residential combustion by 68 % when using daily emissions. A large part (93 %) of this systematic increase can be captured also when using monthly emissions; the increase is compensated by a decreased BC burden at lower latitudes. In a comparison with BC measurements at six Arctic stations, we find that using daily-varying residential combustion emissions and introducing gas flaring emissions leads to large improvements of the simulated Arctic BC, both in terms of mean concentration levels and simulated seasonality. Case studies based on BC and carbon monoxide (CO) measurements from the Zeppelin observatory appear to confirm flaring as an important BC source that can produce pollution plumes in the Arctic with a high BC / CO enhancement ratio, as expected for this source type. BC measurements taken during a research ship cruise in the White, Barents and Kara seas north of the region with strong flaring emissions reveal very high concentrations of the order of 200–400 ng m^{-3}. The model underestimates these concentrations substantially, which indicates that the flaring emissions (and probably also other emissions in northern Siberia) are rather under- than overestimated in our emission data set. Our results suggest that it may not be "vertical transport that is too strong or scavenging rates that are too low" and "opposite biases in these processes" in the

Arctic and elsewhere in current aerosol models, as suggested in a recent review article (Bond et al., Bounding the role of black carbon in the climate system: a scientific assessment, J. Geophys. Res., 2013), but missing emission sources and lacking time resolution of the emission data that are causing opposite model biases in simulated BC concentrations in the Arctic and in the mid-latitudes.

---

1   Introduction

Chemistry transport models (CTMs) and chemistry climate models (CCMs) have large difficulties in simulating high-latitude pollutant concentrations. This is found for pollutant gases with lifetimes on the order of months such as carbon monoxide (CO) but is more severe for shorter-lived species such as aerosols (Shindell et al., 2008). Measured concentrations of accumulation-mode aerosols in the Arctic peak during the winter and early spring, producing the so-called Arctic haze phenomenon (Barrie, 1986; Law and Stohl, 2007). Many CTMs and CCMs, in contrast, have a flat seasonal cycle or even produce a summer maximum in accumulation-mode aerosol concentrations (Shindell et al., 2008). The problems of models to simulate Arctic black carbon (BC) concentrations have recently become a major discussion point, given that BC potentially has a strong influence on radiative forcing in the Arctic, both via direct and indirect effects in the atmosphere and via albedo changes after deposition on snow or ice (Flanner et al., 2007; Quinn et al., 2008; Meinander et al., 2013). Shindell et al. (2008) found a large diversity of results from different models. None of the models could successfully simulate the BC seasonal cycle measured at the Arctic stations Barrow and Alert, and all models strongly underestimated BC concentrations in winter and early spring. A comparison with measured vertical BC profiles in the Arctic also showed large model diversity but almost all models underestimate BC throughout the lower and middle troposphere, whereas some of the models overestimate BC in the upper troposphere and lower stratosphere (Koch et al., 2009). These results indicate severe model deficiencies with respect to simulating Arctic BC concentrations, which also hamper the assessment of the radiative effects of BC in the Arctic (see, e.g., Fig. 5.10 in Quinn et al., 2011).

Hienola et al. (2013) showed evidence for the underestimation of BC emissions from biofuel burning in high-latitude Europe. Most other studies, however, suggest that wet scavenging parameterizations used in the models cause the model problems (e.g., Bourgeois and Bey, 2011; Liu et al., 2012). The buildup of Arctic haze is generally attributed to the inefficiency of removal processes during winter (Shaw, 1995). Garrett et al. (2010, 2011) have argued that seasonal differences in wet scavenging control the aerosol seasonality in the Arctic. Slower transport from source regions in summer also contributes to the seasonal BC minimum (Stohl,

2006) and automatically enhances the effect of wet scavenging due to longer exposure to precipitation en route from the sources to the Arctic than in winter. Indeed, changes in a model's aerosol scheme (i.e., treatment of microphysical properties and atmospheric removal of BC) can change simulated concentrations by more than an order of magnitude in remote regions such as the Arctic (Vignati et al., 2010). Implementing a more realistic aerosol microphysical scheme in one model increased the Arctic BC concentrations near the surface in winter, which is in better agreement with the observations, but at the same time it exacerbated the model overestimates at higher altitudes (Lund and Berntsen, 2012). Another study attributed the transition from high wintertime aerosol concentrations to low concentrations in the summer to the transition from ice-phase cloud scavenging to more efficient warm cloud scavenging, further amplified by the appearance of warm drizzling cloud in the late spring and summer boundary layer (Browse et al., 2012). Also several other recent studies reported improved simulations of Arctic BC surface concentrations after revising the models' aerosol microphysical schemes (e.g., the transformation of BC from a hydrophobic to a hydrophilic state during aerosol aging) and wet scavenging treatment (Liu et al., 2011; Huang et al., 2010a, b; Sharma et al., 2013). We do not question that seasonal changes in BC ageing and/or wet scavenging are important for explaining the seasonal aerosol cycle in the Arctic. However, the recent model revisions were at least partly motivated by deficiencies in simulating Arctic BC and are not always supported by improved process understanding. Bond et al. (2013) noted that "across-the-board adjustments such as altering wet scavenging rates may improve biases in one region but make them worse in another".

In this paper, we explore possible shortcomings in the emission data used in today's CTMs, which may contribute to the difficulties of simulating the seasonality of Arctic aerosol concentrations. In particular, many global models use annually constant emissions, whereas in reality emissions from some source types can vary substantially even from one day to another. For instance, energy requirements for space heating and related residential combustion emissions respond to the daily changes in outside temperatures. Furthermore, to date, emissions from gas flaring by the oil industry have been missing or geographically misplaced in most emission inventories but they are potentially an important source of BC at high latitudes since a significant proportion of total gas flared has been estimated to occur there. For example, in 2008 Russia was responsible for nearly one third of gas flared globally (Elvidge et al., 2009). Here, we will present simulations of BC transport and removal with a Lagrangian model incorporating flaring emissions and daily varying residential combustion emissions to show that simulated Arctic BC concentrations are highly sensitive to these emission sources. We use station and shipboard measurements to show that measurement data can be better explained with our new emission data. This also reduces the need for a drastic and

perhaps unrealistically strong seasonality of wet scavenging in order to reproduce Arctic aerosol concentrations. While the model simulations were done only for BC, the main results of this study should be valid also for other short-lived pollutant aerosols and gases co-emitted by the same sources.

2 Methods

2.1 Emission data

For this study we have used version 4.0 of the ECLIPSE (Evaluating the CLimate and Air Quality ImPacts of Short-livEd Pollutants) project emission data set described in Klimont et al. (2013) and available through the ECLIPSE project website (http://eclipse.nilu.no) upon request. The anthropogenic component of the emission data set used in this work has been developed with the GAINS (Greenhouse gas – Air pollution Interactions and Synergies) model (Amann, 2011, see http://gains.iiasa.ac.at). This model calculates emissions for about 170 regions by all major economic sectors, including energy and industrial production, transport, residential combustion, agriculture, and waste distinguishing several detailed subsectors, fuels, and emission control options. In total, the GAINS model considers nearly 2000 sector-fuel-technology combinations for which emissions are calculated. The GAINS regional BC emission estimates (Klimont et al., 2009; Kupiainen and Klimont, 2007) compare well with other work (e.g., Bond et al., 2004; Zhang et al., 2009; Lu et al., 2011) and are consistent with results from the SPEW model (Bond et al., 2013).

In this paper we focus on the contribution and role of two anthropogenic sources, i.e., residential combustion emissions owing to the assumed significance of their temporal distribution, and on gas flaring emissions due to their increasing relative importance with latitude (Table 1). The GAINS methodology to estimate BC emissions from residential combustion draws on Kupiainen and Klimont (2007). The emission factors aim to reflect real world emissions, i.e., incorporate emission measurements of diluted samples, and have been recently updated for Europe (Boman et al., 2011; Pettersson et al., 2011; Schmidl et al., 2011; Tissari et al., 2008, 2009), specifically for modern stoves and boilers, and Asia (Cao et al., 2006; Chen et al., 2009; Habib et al., 2008; Li et al., 2009; Parashar et al., 2005; Venkataraman, 2005; Zhi et al., 2008, 2009). Activity data on solid fuel combustion in the residential sector originates from the International Energy Agency (IEA, 2011), EUROSTAT, national statistics and contacts with national experts, for example during stakeholder consultation within the revision of the European Union National Emission Ceiling Directive (http://ec.europa.eu/environment/air/review_air_policy.htm) and activities associated with work for the Arctic Council's Taskforce on Short-Lived Climate Forcers (http://www.arctic-council.org). Such consultations have allowed to collect and validate

new information about distribution of various installations (stoves, boilers, pellet stoves, etc.) in several countries.

For gas flaring in the oil and gas industry, GAINS relies on the time series of gas flaring volumes developed within the Global Gas Flaring Reduction initiative (Elvidge et al., 2007, 2011) and emission factors derived on the basis of particulate matter and soot estimates from CAPP (2007); Johnson et al. (2011); US EPA (1995). The current GAINS emission factor for BC ($1.6 \, \mathrm{g \, Nm^{-3}}$ gas flared) is higher than recently proposed values ($0.51 \, \mathrm{g \, Nm^{-3}}$; McEwen and Johnson, 2012). While McEwen and Johnson (2012) consider representative fuel mixtures, their measurements were performed on laboratory-scale flares, which might underestimate real-world emissions. The lack of real field measurements, which should be taken under a large range of operating conditions, makes estimates of BC from this source highly uncertain. However, in our view this does not justify their omission from most of the currently used global data sets. Even when using the emission factor from McEwen and Johnson (2012), gas flaring remains the second largest source of BC emissions north of $60°$ N and the most important anthropogenic source. Although, we are aware of intra-annual variability of flaring emissions, we have no data to support any temporal distribution and assume they are constant through the year.

Emissions from anthropogenic sources other than gas flaring and residential combustion are also included in our emission data set but are treated in the model simulations only at an aggregated level since they are not the focus of this study. For instance, emissions from transport (especially from diesel vehicles) are typically a major source of BC in the developed countries of the Northern Hemisphere (Bond et al., 2004; Kupiainen and Klimont, 2007). These emissions were lumped together with other source categories (industry, waste burning, energy sector excluding flaring) into a single category "other sources". These emissions were held constant over the year.

Open biomass burning emissions were available with monthly resolution from the Global Fire Emissions Database (GFED) version 3.1 (van der Werf et al., 2010). Agricultural waste burning emissions were taken from GAINS and were distributed over the period between 15 March and end of October in the Northern Hemisphere. In summary, we use the following aggregated emission categories for our model simulations:

- residential combustion;

- gas flaring in oil and gas industry;

- on-field agricultural waste burning;

- open biomass burning (forests, grasslands) taken from GFED;

- all other sources (transport, industry, energy sector excluding flaring, waste).

Table 1. ECLIPSE BC emissions (kt/year) for the year 2010 for various lumped source categories. Values are given for the global total emissions, as well as for the emissions north of 40° N, 50° N, 60° N and 66° N. Values in brackets are the relative fractions (in %) of the total emissions in the respective domain.

Emission category	Global		lat > 40° N		lat > 50° N		lat > 60° N		lat > 66° N	
Residential	3055	(38)	472	(36)	93	(17)	6.2	(4)	0.6	(1)
Flaring	228	(3)	83	(6)	69	(13)	52.2	(33)	26.4	(66)
Agricultural waste burning	341	(4)	73	(6)	29	(5)	0.2	(0)	0.0	(0)
Biomass burning	2276	(28)	219	(17)	205	(38)	92.4	(58)	12.3	(31)
Other	2088	(26)	458	(35)	143	(27)	8.0	(5)	1.0	(2)
Total	7988	(100)	1305	(100)	539	(100)	159.0	(100)	40.3	(100)

Aircraft and international shipping emissions have been largely ignored in this study. At the global level, international shipping contributes less than 2 % of BC emissions (Bond et al., 2004; Lack et al., 2008) and their contribution in the Arctic has been estimated for 2004 at about 1 kt BC (Corbett et al., 2010), i.e., less than 1 % of total BC emissions north of 60° N used in this study (Table 1). In the case study presented in Sect. 3.3.2, we use ship emissions as developed for the work on Representative Concentration Pathways (RCP) (Van Vuuren et al., 2011) and find them to be of marginal importance.

The ECLIPSE emission data set does not include any specific information on effective source heights; in view of having no better information, residential and agricultural waste burning emissions were assumed to occur in the lowest 5 m of the atmosphere, flaring emissions between 50 and 150 m above ground level (this shall also account for some inertial and bouyant plume rise), biomass burning emissions between 0 and 100 m, and all other emissions between 0 and 50 m (large combustion plants have typically high stacks but their BC emissions are very small). The emission data were gridded at a resolution of 0.5° latitude × 0.5° longitude and used here for the years 2008, 2009 and 2010.

Figure 1 shows the spatial distribution of BC emissions from the various emission sectors as used in this study for the year 2010, and Table 1 reports the total global emissions for key sectors including their distribution at higher latitudes, i.e., north of 40° N, 50° N, 60° N and 66° N. Major sources of emission at the global level are the residential sector (38 %), biomass burning (28 %) and other sectors (26 %), whereas flaring emissions contribute less than 3 % and agricultural waste burning 4 %. For the Arctic (and especially for the Arctic lower troposphere), however, the high-latitude emissions are more important than global emissions (Stohl, 2006), and in this region the relative contributions are very different. In the ECLIPSE emission data set, biomass burning (58 %) and flaring emissions (33 %) are most important north of 60° N, and north of 66° N flaring emissions (66 %) are dominating. In winter when very little biomass burning occurs, flaring constitutes almost 80 % of the BC emissions north of 60° N, and it is nearly the only source of BC in the

Arctic. The high-latitude flaring emissions occur mainly in the North Sea, the Norwegian Sea, the northeastern part of European Russia and western Siberia. The Russian flaring emissions specifically are located along the main low-level pathway of air masses entering the Arctic (Stohl, 2006), in an area that was also identified as the source region of the highest measured BC concentrations at the Arctic measurement stations Alert, Barrow and Zeppelin (Hirdman et al., 2010). Thus, if the GAINS estimates for the Russian flaring emissions are correct, we might expect this source to be responsible for a large fraction of the BC loadings in the Arctic lower troposphere – something that has not yet received attention in the literature.

Residential combustion emissions are relatively less important at high latitudes than globally but still constitute a major fraction of the total emissions (Table 1). High-latitude residential combustion emissions are concentrated in the winter because they are primarily associated with space heating. The energy demand for heating and the resulting emissions can be quantified using the heating degree day (HDD) concept. This concept assumes that no energy is needed for heating if outside temperatures are above a certain threshold, and that energy demand increases linearly with decreasing temperatures below that level. It has been shown that the fuel use correlates very well with HDDs (Quayle and Diaz, 1980). With a base temperature of 15 °C, the HDDs are given by $H_{dd} = 15 - T$, where T is the outside daily average air temperature in degree Celsius. Since we implement this concept using 3-hourly two-meter temperatures from the European Centre for Medium-Range Weather Forecasts (ECMWF), we calculate $H_{dd,j}^{3h} = \frac{3}{24}(15 - T_j^{3h})$ for the 3 h period j. For an emission grid cell with annual emission E^a, we calculate the total annual sum of HDDs, H_{dd}^a, in that cell and then distribute the annual emissions to 3-hourly periods according to $E_j^{3h} = E^a \frac{H_{dd,j}^{3h}}{H_{dd}^a}$. That means we scale the annual BC emissions from the GAINS inventory with the 3-hourly HDD values, to derive an emission data set that is consistent with annual GAINS estimates but with a 3 h time resolution. We also calculate monthly emissions based on the monthly sums of HDDs.
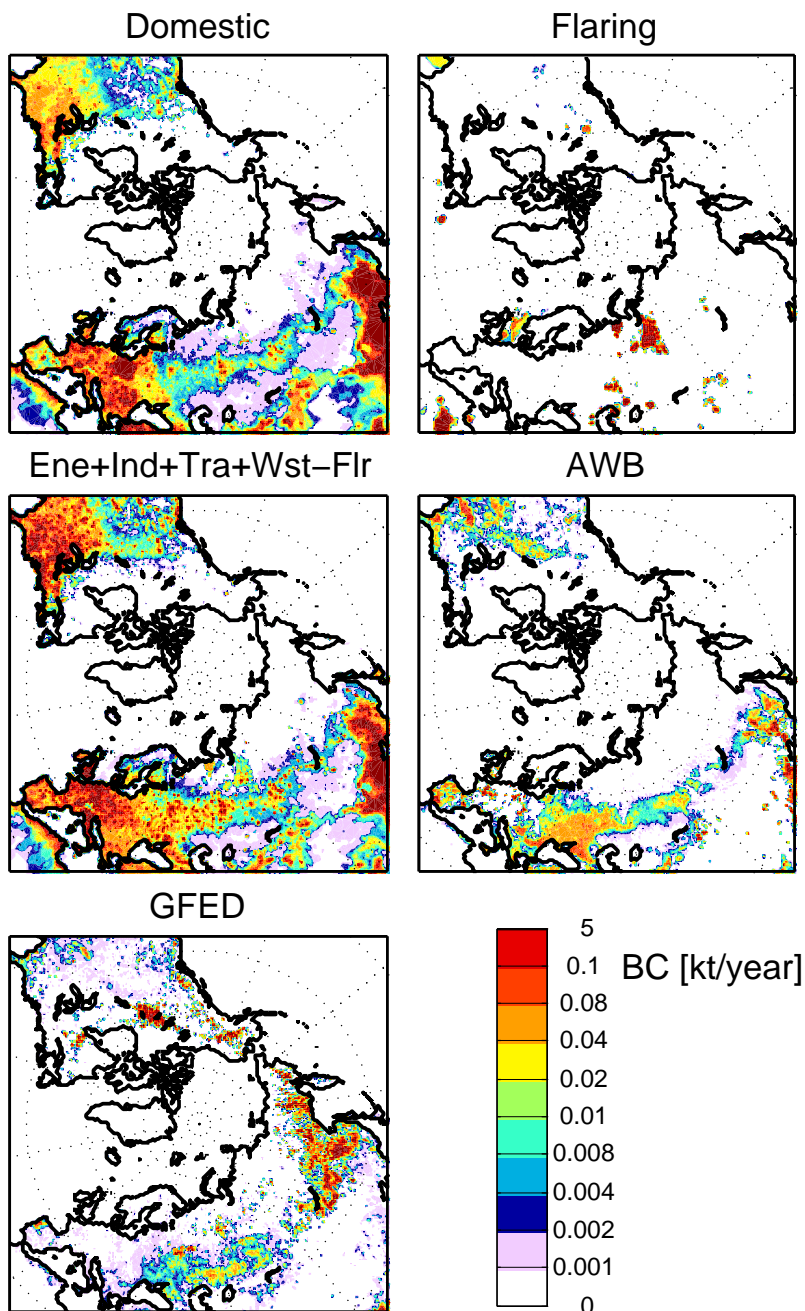
Fig. 1. Annual BC emissions (average over the period 2008–2010) from different emission sectors: residential combustion emissions (top left), flaring emissions (top right), emissions from the lumped sectors energy excluding flaring, industry, traffic, waste burning (middle left, marked "Ene+Ind+Wst-Flr"), agricultural waste burning (middle right, marked with "AWB"), and GFED biomass burning emissions (bottom left).

Residential BC emissions occur not only from space heating but also from cooking. The latter is of high relevance at lower latitudes. We assume that north of 55° N, residential combustion emissions are entirely due to space heating, whereas south of 15° N, emissions are independent of outside temperature and, thus, constant throughout the year. Between 15 and 55° N, we apply a linear weighting depending on latitude between heating and other emissions. We consider this simple approach sufficient for our sensitivity studies, since we are interested in the higher latitudes where space heating is dominant. More sophisticated approaches will be needed

to fully capture temporal variability of residential combustion emissions of BC on a global scale.

Figure 2 shows the resulting seasonal cycle of residential combustion BC emissions averaged over the years 2008–2010 for four different latitude bands. For the latitudes 55–65° N, emissions in January are nearly 40 times higher than in July, whereas for the lower-latitude bands, the seasonal cycle is less strong. Emissions north of 65° N are very small compared to those at lower latitudes and their seasonal cycle is also weaker than for the 55–65° N band because relatively cold temperatures can also occur in summer.

In Sect. 3.3.2, we use measurements of BC and CO to discuss the contribution of gas flaring emissions to measured BC. Therefore, it is important to know the expected emission ratio of BC/CO for gas flaring and for other sources. While there is a large range of reported BC/CO emission ratios for individual sources, at an aggregated regional level residential combustion has BC/CO emission ratios of typically about 0.02–0.03, transportation of about 0.004–0.02 depending on share of diesel vehicles, and open biomass burning of about 0.01. For gas flaring, we estimate a much higher BC/CO emission ratio in the range of 0.05–0.5. However, actual measurements of emission factors for gas flaring are sparse and are often available for single pollutants only, making it difficult to infer emission ratios. A study by the Canadian Association of Petroleum Producers (CAPP, 2007) has derived a BC/CO ratio of about 0.3, which is at least an order of magnitude higher than for most other BC sources at an aggregated regional level. Few studies report very low BC/CO ratios for flaring, of the order of 0.004 (EEA, 2009; Plejdrup et al., 2009) but these are actually $PM_{2.5}$/CO ratios and it is not clear whether these measurements were actually performed on the same flares. Furthermore, the given $PM_{2.5}$ emission factors are much lower than the most recent soot measurements (McEwen and Johnson, 2012). In summary, the possible BC/CO emission ratio range for flaring is large and remains uncertain, however, it is most likely larger than for other key BC-emitting sectors. CO has a lifetime in the atmosphere of several weeks to months (with the longest lifetimes in the Arctic in winter) and is therefore often used as a tracer of polluted air masses. A high measured enhancement ratio of BC / ΔCO (where ΔCO is the measured CO enhancement over background levels) may thus indicate a large flaring contribution to measured BC. We will use this indicator in Sect. 3.3.2 for source attribution.

2.2 Model simulations

We simulated the concentrations of BC with the Lagrangian particle dispersion model FLEXPART (Stohl et al., 1998; Stohl and Thomson, 1999; Stohl et al., 2005) using three-hourly operational meteorological analyses from the European Centre for Medium-Range Weather Forecasts (ECMWF) with 91 model levels and a horizontal resolution of 1° × 1°. We ran FLEXPART with tagged tracers for each one of the different emission categories discussed in Sect. 2.1. Computational particles were randomly generated in the 0.5° × 0.5° emission grid boxes according to the 3-hourly (subsumed into daily resolution), monthly, or annual mean emission mass fluxes, depending on the model experiment. The particles were tracked forward in time and were dropped from the simulation after 31 days. Each simulation was run for the period 2008–2010 and produced daily output with a resolution of 1° latitude × 2° longitude.

We simulate three different BC-like tracers: one with a fixed 3 day lifetime, one with a fixed 10 day lifetime, and one aerosol tracer, which is subject to removal processes. For the aerosol tracer we assumed a particle density of $1400\,\mathrm{kg\,m^{-3}}$ and a logarithmic size distribution with an aerodynamic mean diameter of $0.25\,\mu m$ and a logarithmic standard deviation of 1.25. These values are used by FLEXPART's dry deposition scheme, which is based on the resistance analogy (Slinn, 1982). For the wet deposition, FLEXPART considers below-cloud (McMahon and Denison, 1979) and within-cloud scavenging (Hertel et al., 1995). The below-cloud scavenging coefficient $\Lambda = AI^B$ increases with precipitation rate I, where $A = 2 \times 10^{-7}\,\mathrm{s^{-1}}$ is the scavenging coefficient at $I = 1\,\mathrm{mm\,h^{-1}}$ and $B = 0.62$. The in-cloud scavenging depends on cloud liquid water content, precipitation rate and the depth of the cloud. For more details on aerosol removal parameterizations, see Stohl et al. (2005) and the FLEXPART user manual available from http://www.flexpart.eu. The simulated average concentrations of the aerosol tracer are slightly lower than for the 10 day lifetime tracer. A lifetime of almost 10 days is longer than the global lifetime of accumulation-mode aerosols in most models (Textor et al., 2006) which, however, may be too short (Kristiansen et al., 2012).

FLEXPART does not simulate aerosol chemistry and microphysics and treats BC in a simplified way. The conversion of BC from a hydrophobic to a hydrophilic state and changes in the aerosol size distribution are ignored. The wet scavenging coefficients used in the simulations are more typical for a hydrophilic aerosol and therefore the removal of BC close to its sources is likely overestimated. Furthermore, as particles are removed from the simulation after 31 days, small contributions to the atmospheric BC burden from very aged BC tracer are missed. In that respect, our simulations are much less realistic than calculations with more sophisticated aerosol models. However, advantages are the good accuracy of the simulated transport and the lack of numerical diffusion, which is particularly important in the very stable Arctic atmosphere. Furthermore, our goal here is not to achieve the most realistic simulation of global BC but only to explore the sensitivity of Arctic BC to changes in the emission treatment, and for that purpose, we believe our model setup is realistic enough.

For case studies (Sects. 3.3.2 and 3.3.3), we also ran FLEXPART backward in time, in so-called "retroplume" mode (Stohl et al., 2003) from a measurement location, to
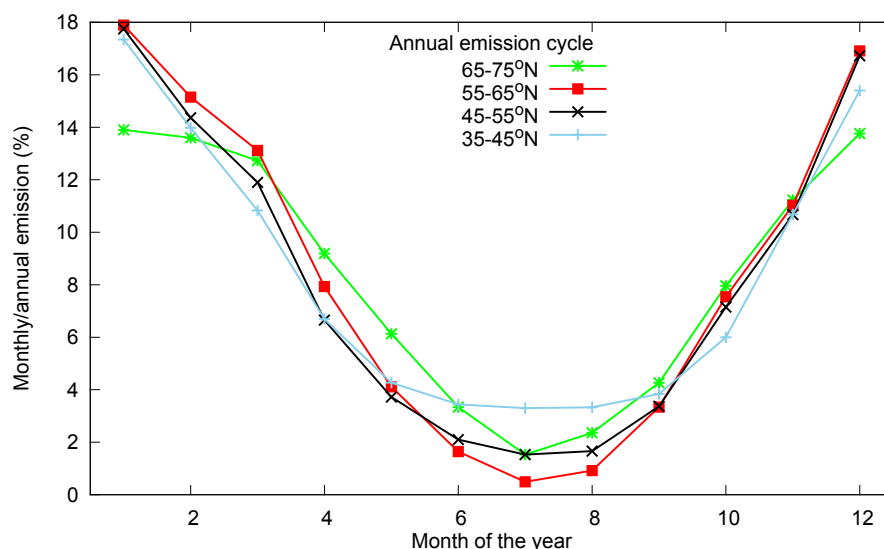
Fig. 2. Monthly BC emissions from the residential combustion sector relative to total annual emissions from this sector based on the HDD concept and averaged over the years 2008–2010, for the four latitude bands 35–45° N, 45–55° N, 55–65° N and 65–75° N.

identify the source region of measured BC. The FLEXPART retroplume output is an emission sensitivity which, when multiplied with emission fluxes, yields a simulated concentration at the receptor. For the simulations we have used the same tracer properties as for the forward BC aerosol tracer, which means that removal processes are accounted for also in backward mode. In addition to allowing identifying the BC source regions, our backward simulations also have the advantage that they were initialized at the measurement point (rather than a grid cell) and that they were started every three hours and carried many particles (80 000 each), thus minimizing statistical sampling uncertainty.

2.3 Measurement data

We compare our model results with measurements of aerosol light absorption from six sites located in different parts of the Arctic: Barrow, Alaska (156.6° W, 71.3° N; 11 m a.s.l.), Alert, Canada (62.3° W, 82.5° N; 210 m a.s.l.), Pallas, Finland (24.12° E, 67.97° N; 565 m a.s.l.), Zeppelin/Ny Ålesund, Spitsbergen, Norway (11.9° E, 78.9° N; 478 m a.s.l.), Station Nord, Greenland (16.67° W, 81.6° N; 30 m a.s.l.) and Summit, Greenland (38.4° W, 72.6° N; 3208 m a.s.l.). Different instruments were used at these sites: an aethalometer at Summit, particle soot absorption photometers (PSAPs) at Barrow, Alert, Station Nord and Zeppelin, and a multi-angle absorption photometer at Pallas (Hyvärinen et al., 2011). These instruments measure the particle light absorption coefficient σ_{ap}, each at its own specific wavelength (typically at around 530–550 nm), and for different size fractions of the aerosol (typically particles smaller than 1, 2.5 or 10 μm are sampled). Conversion of σ_{ap} to BC mass concentrations is not straightforward and requires certain assumptions. The

mass absorption efficiency used for conversion is site, instrument and wavelength specific and uncertain by at least a factor of two. For the aethalometer at Summit, this conversion is done internally and we directly use reported mass concentrations. For Station Nord, a mass absorption efficiency of 3.9 m² g⁻¹ multiplied by a filter constant of 2 was used for conversion, based on comparison to elemental carbon measurements (Nguyen et al., 2013). For the other sites, we convert the measured light absorption to BC mass concentration using a mass absorption efficiency of 10 m² g⁻¹, typical of aged BC aerosol (Bond and Bergstrom, 2005). Sharma et al. (2013) used the even higher value of 19 m² g⁻¹ for Barrow and Alert data. We refer to the converted light absorption values as equivalent BC (EBC) to reflect the uncertainties in this conversion, as well as other uncertainties resulting for instance from the use of different cut-off sizes for the different instruments.

For all stations except for Summit and Station Nord we had data available for the years 2008–2010, corresponding to the modeling period. For Summit, we used the data set produced by Hirdman et al. (2010), where influence from local pollution sources (mainly a diesel generator) was removed by filtering the data according to wind direction. These data were, however, only available until fall 2008, so we used the years 2005–2008. Measurements at Station Nord started only in March 2008 and data capture was low in some other months of the year 2008, so we used data only from the years 2009–2010. Barrow and Alert data are routinely subject to data cleaning, removing the influence from local sources. Zeppelin generally is not strongly influenced by local emissions; however, summer values are enhanced by some 11 % due to local cruise ship emissions (Eckhardt et al., 2013).

For case studies, we also use CO data from the Zeppelin station. CO was measured using a RGA3 analyzer (Trace Analytical) fitted with a mercuric oxide reduction gas detector. Five ambient air measurements and one field standard were performed every 2 h. The field standards were referenced against the CO WMO2000 reference scale maintained at National Oceanic and Atmospheric Administration/Earth System Research Laboratory (NOAA/ESRL). This scale was designated by WMO as the reference scale for the Global Atmospheric Watch (GAW) program (WMO, 2010).

EBC was also measured onboard of the research vessel *Akademik Mstislav Keldysh* during a cruise in the White, Barents and Kara seas from 12 September until 7 October 2011. Aerosol samples were collected on the foredeck over 10–14 h periods by sucking air through perchlorovinyl fiber filters and avoiding contamination by the ship exhaust. The filters were subsequently analyzed using aethalometry by a custom-built photometer constructed by one of the co-authors (V. Kopeikin) in close collaboration with A. Hansen (Magee Scientific, USA). The instrument was calibrated together with A. Hansen and the Institute of Atmospheric Optics (Tomsk, Russia). A mass absorption efficiency of $21 \, \mathrm{m^2 \, g^{-1}}$ was used in this case for converting σ_{ap} to EBC mass concentrations (Hansen et al., 1984).

3 Results

3.1 Time resolution of residential combustion emissions

The top panel in Fig. 3 shows a map of the annual mean surface concentrations of the BC aerosol tracer for residential combustion emissions when these emissions are held constant over the year. The resulting BC concentrations are highest in Eastern Asia, followed by Europe and eastern North America. The concentrations are lowest in the Arctic. The middle panel in Fig. 3 shows the relative concentration changes when the residential combustion BC emissions are resolved by month using the HDD concept instead of keeping the emissions constant throughout the year. In this case the high-latitude emissions are concentrated during the winter months (see Fig. 2). During winter the transport from the major Eurasian source regions towards the Arctic is much stronger than during summer when the Arctic is almost isolated from the middle latitudes (Stohl, 2006), and the BC removal is also weaker in winter than in summer. This causes not only a strong increase of simulated BC concentrations in the Arctic lower troposphere in winter, but also a systematic 60–100 % enhancement even of the annual mean simulated concentrations throughout most of the Arctic (Fig. 3, middle panel). The enhancement averaged over the Arctic north of 66° N is 63 %.

To explore whether daily resolution of the emission data causes further changes, we plot in the bottom panel in Fig. 3 the resulting relative difference in annual mean concentra-
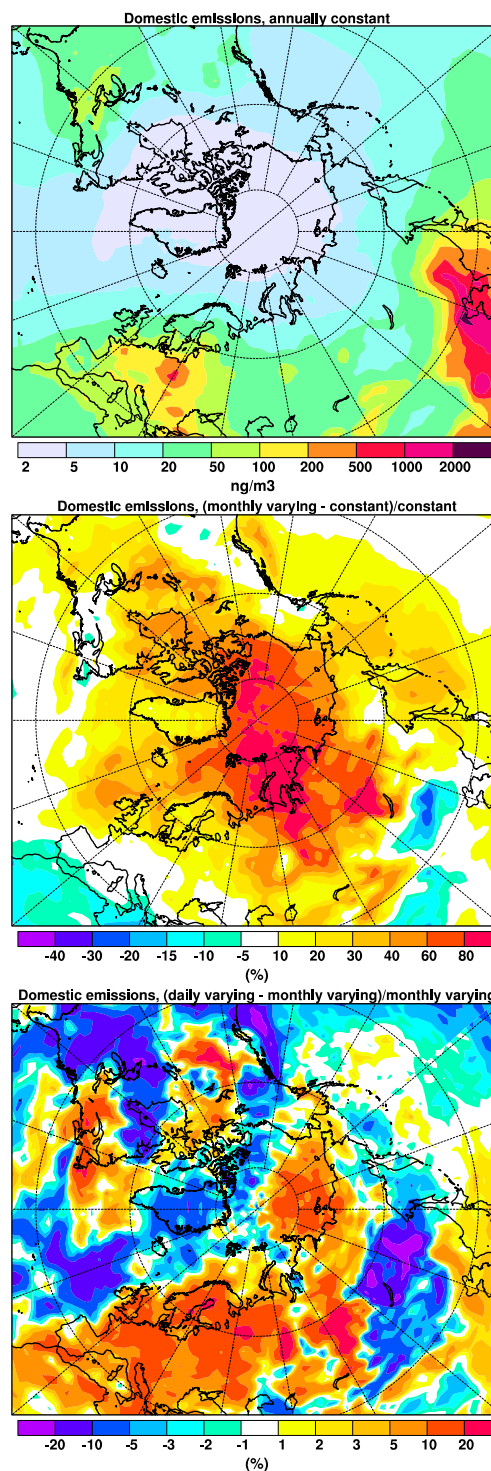

Fig. 3. Annual mean surface concentrations of the BC aerosol tracer for annually constant residential combustion emissions (top), relative difference between the BC aerosol tracer surface concentrations for monthly varying versus annually constant residential emissions (middle) and relative difference between the BC aerosol tracer surface concentrations for daily varying versus monthly varying residential emissions (bottom).

tions when using emission data with daily and with monthly resolution. In this case, the relative differences are smaller but over northern Eurasia the concentrations are further enhanced by some 10 % when using daily emission resolution. Overall, for daily resolved residential combustion emissions, the annual mean enhancement for the Arctic north of 66° N compared to annually constant emissions is 68 %, compared to the 63 % enhancement when using monthly mean emissions. The reason for this further enhancement is that temperatures in winter are coldest and heating emissions highest on days with stagnant conditions when the BC emissions remain close to the ground. Furthermore, these cold air masses have a greater probability of entering the so-called polar dome (Klonecki et al., 2003; Stohl, 2006) or are already inside the dome, which means they can be transported polewards near the surface. This explains why the largest enhancements are seen north of the major emission areas and why they extend into the Eurasian part of the Arctic. It is also important to notice that the enhancements in winter are much larger than the annual mean enhancements. The strongest enhancements occur in January when Arctic-mean surface concentrations of residential combustion BC are enhanced by 150 % compared to when annually constant emissions are used. This is partly compensated by reduced concentrations in summer, leading to large changes in the simulated annual cycle of BC (see Sect. 3.3.1).

Figure 4 shows vertical profiles of the residential combustion BC aerosol tracer, averaged over the Arctic region, for the months of January and July. In January, the vertical profiles show a maximum a few hundred meters above the surface, whereas in July the maximum occurs in the mid-troposphere. The decrease towards the surface in the lowest 1 km is partly related to dry deposition. It is weaker but still present for the tracers with fixed lifetime (not shown), in this case a result only of the quasi-isentropic tracer uplifting. Allowing the emissions to vary by month dramatically increases the tracer concentrations in winter throughout the troposphere but with largest absolute increases in the lower troposphere, compared to the case with constant emissions throughout the year. Allowing the emissions to further vary by day instead of per month increases the concentrations in the lowest few hundred meters even more, but slightly reduces the concentrations higher up. In summer, in contrast, the concentrations are strongly reduced throughout the troposphere when emissions are allowed to vary by day or – especially – by month compared to the constant emissions. Notice that daily emission variations lead to a relatively strong relative increase of the Arctic summer BC concentrations from residential combustion compared to monthly emissions, again because of preferential poleward transport of colder air masses containing heating emissions. The net effect over the year of the daily varying emissions is a 68 % increase of the annual mean tracer concentrations near the surface, as already seen in Fig. 3. In contrast, in the upper troposphere

the annual mean concentrations are reduced, e.g., by 25 % at 8000 m a.s.l.

The annual mean BC tracer deposition fluxes from annually constant residential combustion emissions are shown in the top panel of Fig. 5 and the relative changes when using daily varying emissions are shown in the bottom panel. The relative deposition differences are close to zero in the BC source regions. Increases of about 20–50 % are found north of Europe when using daily varying emissions, whereas decreases occur in northeastern Asia and northwestern North America. In the Arctic, the differences are generally positive but smaller than surface concentration differences (compare with Fig. 3). The reason for these less systematic and overall smaller changes is that most of the deposition in the model (ca. 95 %) is due to wet scavenging, which can occur throughout the depth of the atmosphere, and average concentrations in the upper troposphere are actually higher when emissions do not vary (Fig. 4). Results for monthly varying emissions are similar to those for daily emission variation (not shown).

3.2 The importance of flaring emissions

Figure 6 shows the annual mean total simulated surface concentrations of the BC aerosol tracer from all emission sources (Fig. 6, top left) as well as the relative contributions from the various simulated emission categories. In accordance with their large fraction of total emissions (see Table 1), residential combustion emissions (daily resolved) contribute more than 30 % of the total simulated surface concentrations in large parts of the Northern Hemisphere (Fig. 6, top right). Even in the Arctic, contributions exceed 20 % almost everywhere and over Scandinavia exceed even 40 %. In contrast, agricultural waste burning and biomass burning emissions (Fig. 6, middle) contribute relatively little to the Arctic annual mean BC concentrations, given their large fraction (especially of the biomass burning emissions) of the total emissions north of 50° N. The reason for this is that these emissions occur mainly from spring to early fall, when transport into the Arctic lower troposphere is limited. However, when only summer is considered, biomass burning emissions dominate the total BC loading in the Arctic (see lower panel of Fig. 7, which will be discussed later).

Of greatest interest here is the contribution from flaring emissions (Fig. 6, bottom left). While in our emission data set they make up for less than 3 % of the total global BC emissions (Table 1), their contribution to simulated surface concentrations exceeds 20 % over all of the Arctic Ocean. In fact, the average modeled flaring contribution to the annual mean BC surface concentrations north of 66° N is 42 %, with a seasonal peak of 52 % in March. In summary, flaring emissions contribute more to the Arctic surface concentrations of BC than any other emission category, including our lumped category "other emissions" (energy sector without flaring, industry, traffic, waste), also shown in Fig. 6 (bottom right).
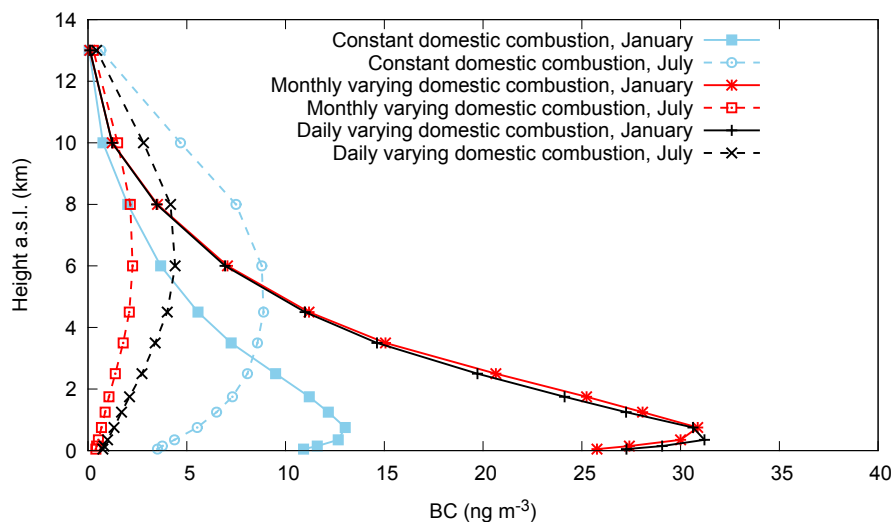
Fig. 4. Vertical profiles of the BC aerosol tracer from residential ("domestic") combustion averaged for the Arctic area north of 66° N for the months of January (solid lines) and July (dashed lines) when emissions are held constant over the year (light blue lines), varied by month (red lines) or varied daily (black lines) according to the HDD concept.

In January, residential combustion, flaring and all other emissions contribute similar fractions to the total simulated surface concentrations of BC in the Arctic, and the concentrations of all these tracers decrease quickly with altitude (Fig. 7, top). The decrease with altitude is, however, most pronounced for the flaring tracer, which is almost exclusively found below 2 km a.s.l. This is a consequence of the high-latitude source region of this tracer, which limits isentropic lifting in the polar dome (Stohl, 2006). In July, BC concentrations throughout the Arctic troposphere are dominated by biomass burning emissions (Fig. 7, bottom), which peak at about 2–3 km altitude. Notice also the reversed seasonal cycle of Arctic BC at higher altitudes (summer maximum) compared to the surface (winter maximum).

With respect to the BC deposition in the Arctic, the spatial patterns of the relative contributions of the various tracers are similar to those of the surface concentrations shown in Fig. 6. The flaring tracer is somewhat less important for the deposition than for the surface concentrations, due to its rather limited vertical extent, but it still contributes more than 30 % to the simulated BC deposition north of 80° N (not shown). Daily varying residential combustion emissions also contribute more than 30 % in most of the central Arctic, a somewhat larger contribution than to the surface concentrations (not shown). The other tracers contribute with similar fractions to the BC deposition as to the surface concentrations.

3.3 Comparison with measurement data

3.3.1 Seasonality

When comparing modeled and measured concentrations, it is important to bear in mind that the measured EBC concentrations are uncertain by at least a factor of two, and that the model treats BC in a simplified way and misses ship and aircraft emissions. Still, it is interesting to compare the seasonal cycle of measured EBC and modeled BC at the Arctic stations (Fig. 8). Notice also that there is very strong interannual variability in both the measured and modeled monthly means, which we do not discuss any further. For reasons of clarity (the vertical axes would need to be extended considerably), we also refrain from indicating this variability in Fig. 8.

At Barrow and Alert (top panels in Fig. 8), the model underestimates the measured concentrations from January to May and, especially at Barrow, overestimates the measured concentrations in summer. The overestimation is due to a large contribution from biomass burning in summer, which is obviously not seen in the Barrow measurement data. In an earlier study (Stohl et al., 2006), we have found that biomass burning plumes were unintentionally excluded by the local pollution data screening done for Barrow, which removes pollution plumes arriving from the land. When removing the data cleaning, there is indeed a noticeable increase in the measured values in summer, for instance by more than a factor of two in July and more than a factor of three in August, leading to a secondary maximum in measured EBC values at Barrow during July and August (J. Ogren, personal communication, 2013). This is consistent with the modeled biomass burning peak during these months, although the modeled
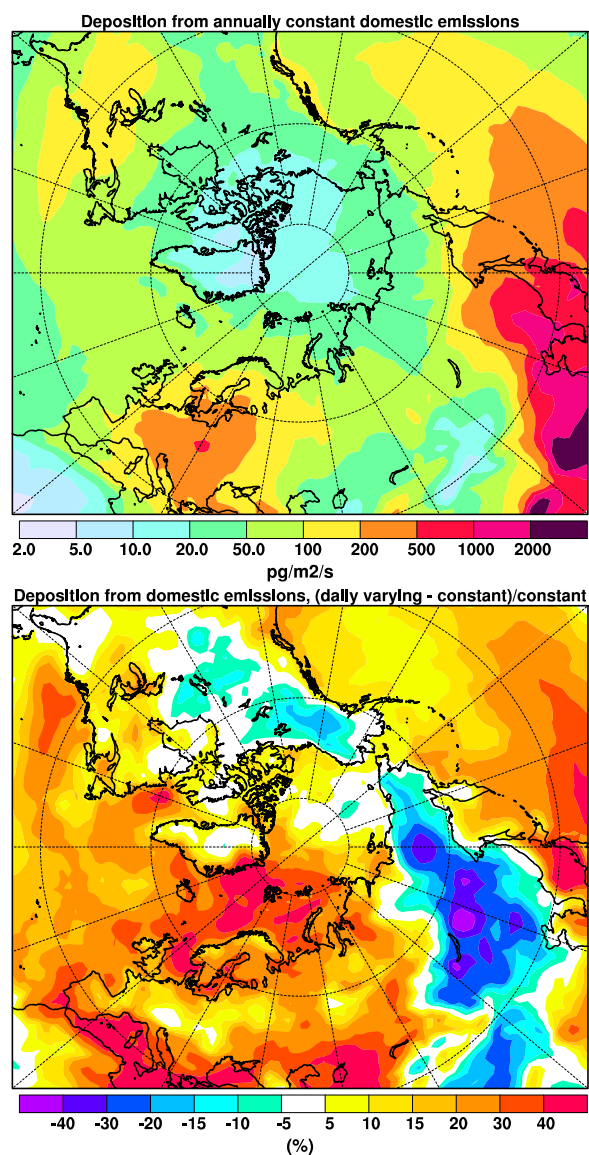
Fig. 5. Annual mean surface deposition of the BC aerosol tracer for annually constant residential combustion emissions (top), and relative difference between the BC aerosol tracer surface concentrations for daily varying versus annually constant residential emissions (bottom).

peak remains too strong compared to the measured one. Both at Alert and Barrow the modeled seasonality of BC concentrations is not strong enough. The seasonality would be even weaker without daily variation of the residential combustion emissions (compare red-shaded area with blue line) and without the flaring emissions (brown-shaded area).

At Pallas and Zeppelin (middle panels in Fig. 8), both the measured and modeled EBC concentrations in winter and spring are higher than at Barrow and Alert. At these stations, the modeled seasonality is of about the right magnitude but

concentrations at Zeppelin in spring are underestimated, and concentrations both at Zeppelin and Pallas in fall are overestimated. At these two sites the residential combustion emissions contribute more than 50 % to the modeled winter concentrations. With annually constant emissions, however, the seasonal cycle would be too weak and winter concentrations would be clearly underestimated. Measured EBC at Zeppelin peaks in March, which is one month later than at Barrow and two months later than at Alert and Pallas. Interestingly, the modeled BC at Zeppelin has a strong contribution from flaring emissions and this contribution is largest in March. While the model fails to capture the March peak, this discrepancy would be even larger without the flaring emissions.

At the remote Station Nord (bottom left panel in Fig. 8) both measured and modeled concentration levels are lower than at the other surface sites. The measurements show a distinct peak in April which, however, is due only to a very high observed monthly mean in the year 2009 ($61 \, ng \, m^{-3}$), whereas the corresponding value in 2010 was much lower ($16 \, ng \, m^{-3}$). The model captures the overall concentration levels quite well, but overestimates the very low measured concentrations in summer substantially, likely because of an overestimated biomass burning impact. The impact of flaring emissions is relatively weak at Station Nord but it is again largest in spring, which helps explaining the measured spring peak. The time-varying residential combustion emissions lead to an improved simulated seasonality as well.

At Summit (bottom right panel in Fig. 8), both the measured and modeled (E)BC concentrations in winter and early spring are much lower than at the other sites, except for Station Nord. From May to August, the measured concentrations fluctuate strongly, with large differences between the different years (not shown). During this period, the model shows a large contribution from biomass burning, which also varies strongly between different years. However, since the measurements and model results are from different years, it is probably not surprising that the model does not match the measured seasonality. An important reason for the modeled concentrations being lower at Summit than at the other stations is that, due to the station's high altitude, the contributions from flaring emissions throughout the year and from residential combustion emissions in winter are much lower, which seems to agree with the measurements. Summit measurements also seem to confirm that the modeled transition in the Arctic to a reversed seasonal cycle of BC at higher altitudes compared to the surface is real.

Summarizing our comparisons of modeled versus measured BC seasonality, the model generally captures the differences at the different stations in seasonality and concentration levels. However, not all features of the observations are perfectly reproduced by the model, and it is likely that remaining disagreements are mainly due to our rather simple treatment of BC removal processes. However, for all stations the results are improved by introducing time variation for the residential emissions and by adding the flaring emissions.
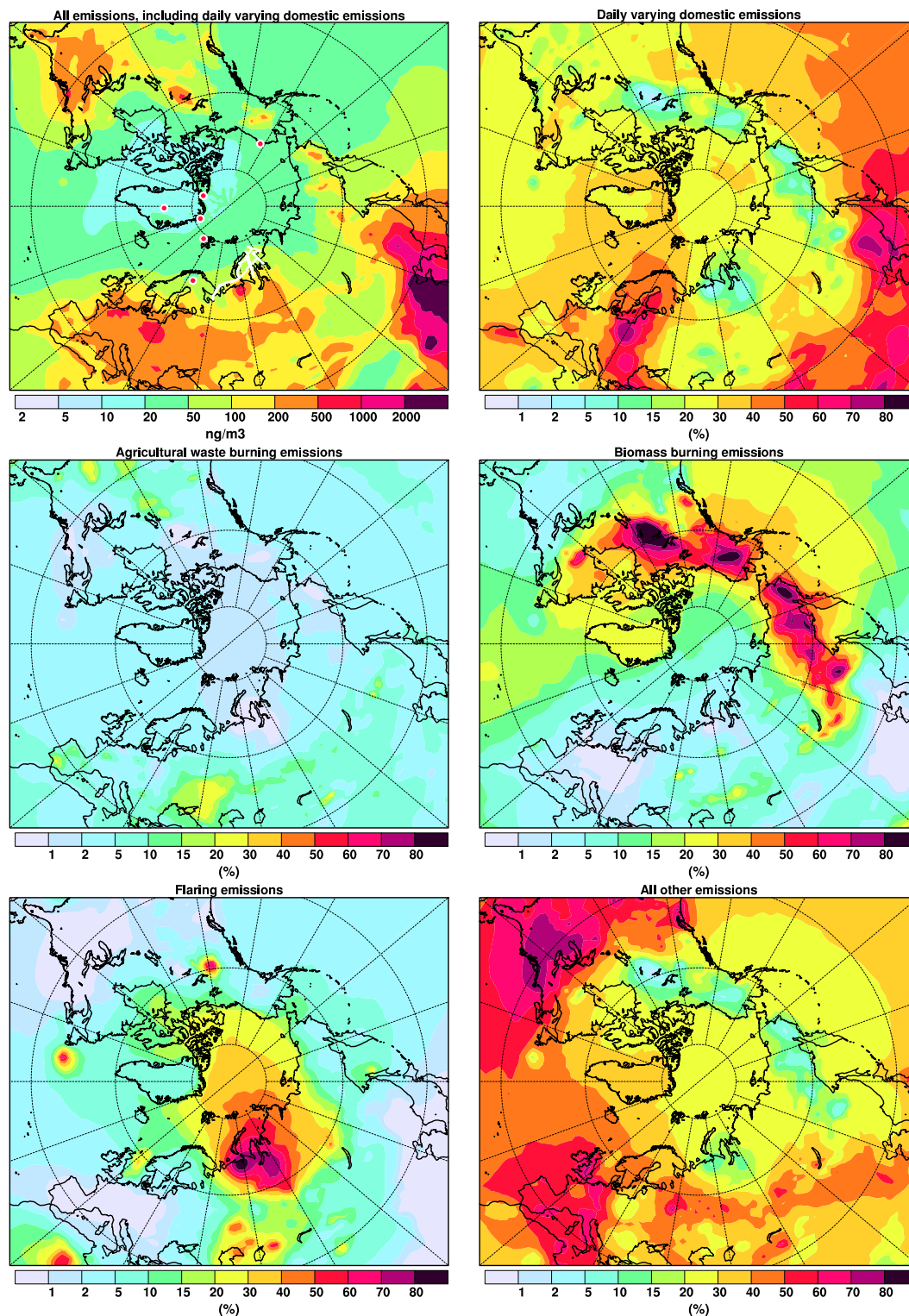
Fig. 6. Simulated annual mean surface concentrations (ng m^{-3}) of the BC aerosol tracer from all emission categories (top left) as well as relative contributions (%) from the various simulated emission categories: residential combustion emissions (top right), agricultural waste burning emissions (middle left), biomass burning emissions (middle right), flaring emissions (bottom left) and all other emissions (bottom right). In the top left panel, the locations of measurement stations discussed in Sect. 3.3.1 are marked with white dots with smaller red dots on top, and the track of the research vessel *Akademik Mstislav Keldysh* is marked with a white line.
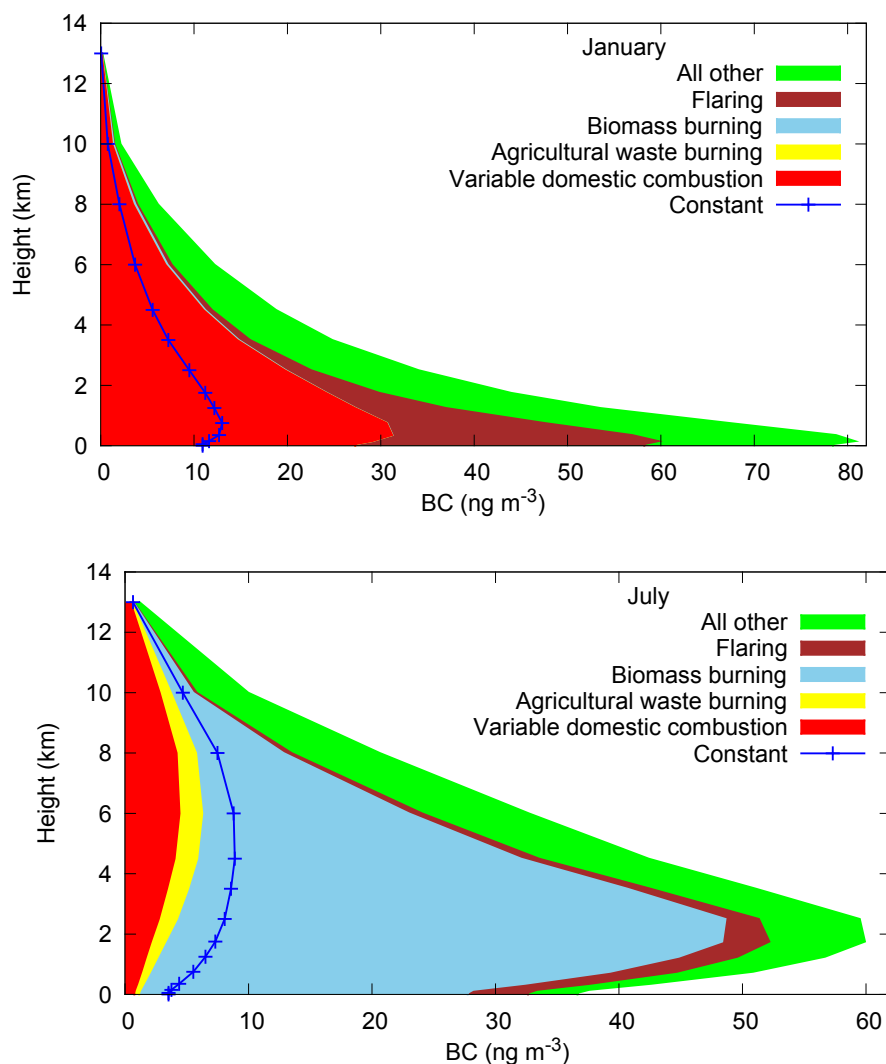
Fig. 7. Vertical profiles of the BC aerosol tracer averaged for the Arctic area north of 66° N and split according to source category for January (top) and July (bottom). The blue line with plus symbols shows the vertical profile of the residential ("domestic") combustion tracer with constant emissions.

3.3.2 Zeppelin station case study of flaring impact

Figure 8 suggests that the Zeppelin station offers the best chances of directly attributing measured EBC to flaring emissions. For detailed analyses, we selected periods when the modeled flaring contribution from the backward simulations was large. While many such episodes were found, most of them are associated also with strong simulated contributions from other BC sources, making it difficult to disentangle the various BC contributions based on measured concentrations. As an example, Fig. 9 shows data from the period 12 February until 4 March 2010, when three different pollution episodes occurred. From 12–14 February, the model simulates up to 140 ng m^{-3} BC, while the measured EBC concentrations are considerably lower. According to the FLEX-

PART retroplumes (not shown), the source region during this period is shifting from Scandinavia and eastern Europe to the European part of Russia. Measured mixing ratios of CO are relatively high during this period. CO is emitted by combustion sources and has a lifetime of months in the atmosphere, thus tagging air masses that were influenced by combustion sources. The low measured EBC concentrations suggest that wet scavenging was important for removing most of the BC that was likely co-emitted with CO. The model seems to have underestimated the wet removal in this case.

During the period 15–17 February the source area of the sampled air mass is centered on the region in high-latitude Russia with strong flaring activity (see Fig. 1). The emission sensitivity footprint, however, is large, with substantial BC contributions coming even from south of 50° N. The
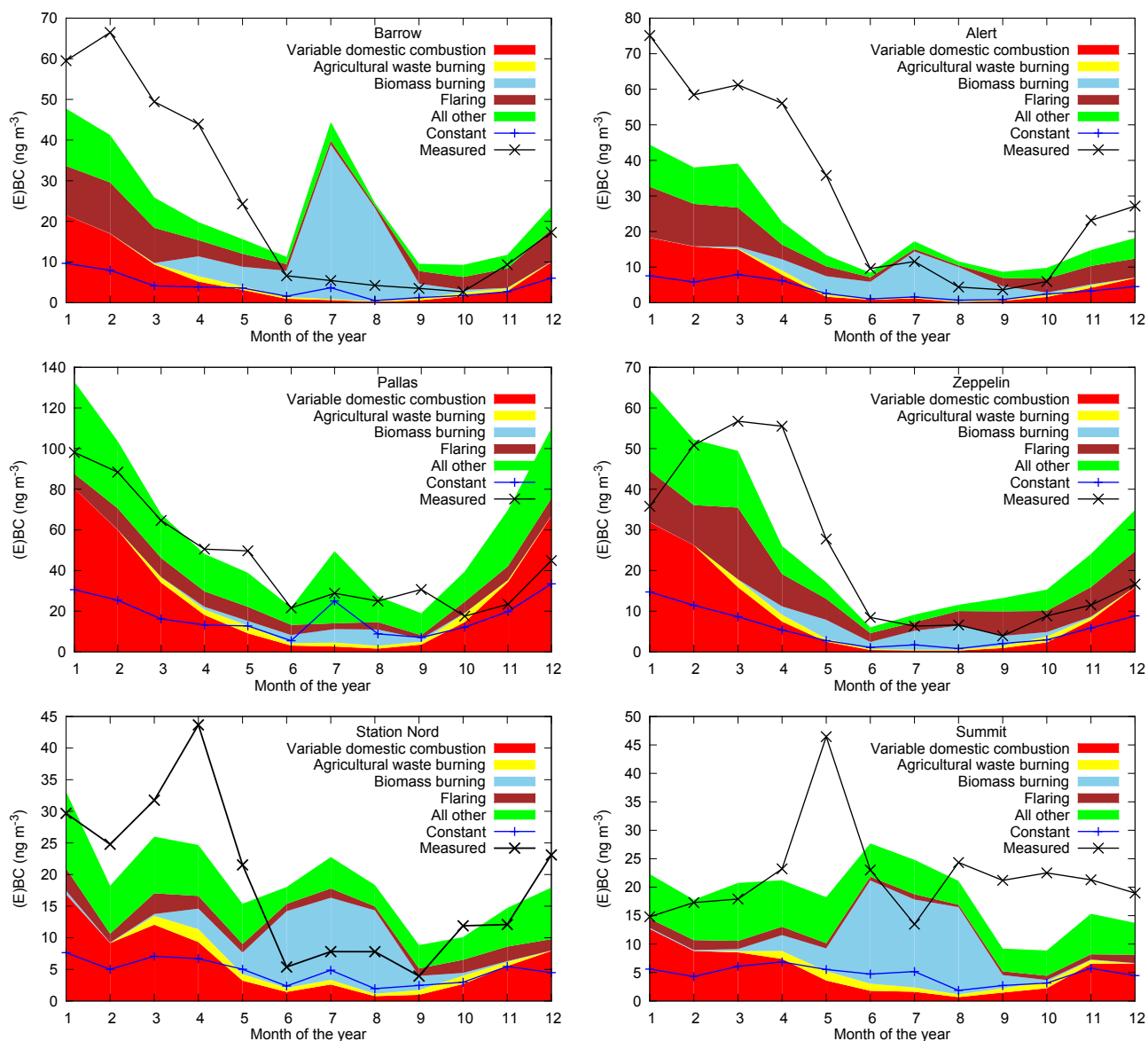
Fig. 8. Comparison of monthly mean modeled BC and measured EBC concentrations at Barrow (top left), Alert (top right), Pallas (middle left), Zeppelin (middle right), Station Nord (bottom left) and Summit (bottom right). The measurements are shown with a black line with crosses, whereas the model results are split into contributions from different sources according to the color legend. Also shown are the results for the residential ("domestic") combustion tracer with constant emission rate throughout the year (blue line with plusses), which can be compared directly with the variable emission tracer (red area). Data shown are averages for the years 2008–2010, except for Summit where the measurement data were averaged over the years 2005–2008, and Station Nord where measurement data were averaged over the years 2009–2010. Notice that scales are different for the different panels.

measured EBC concentrations during this period reach almost 200 ng m^{-3}. It is likely that this includes a substantial flaring contribution, since the measured peak coincides with the time of the largest modeled flaring contribution (Fig. 9). Notice that the peak in measured CO is much broader than the EBC peak and that the two highest measured EBC concentrations actually coincide with small local dips in CO. This suggests a large contribution from a source with a high

BC / CO emission ratio during the time of the measured EBC peak. As we have discussed in Sect. 2.1, gas flaring likely is such a source.

From 20–26 February, the source region of the air mass sampled at Zeppelin is mainly the Arctic Ocean and simulated BC as well as measured EBC and CO are very low most of the time. On 24 February, there was a temporary shift in simulated transport as the air arrived directly from

the western region of intense flaring. The FLEXPART foot-print emission sensitivity was high above the gas flaring region but the retroplume did not extend over any other major BC source region (Fig. 10). Accordingly, the model shows a short spike in simulated BC, which is almost exclusively due to flaring emissions. The measured EBC peaks exactly at the same time and is of a similar magnitude as the model tracer, while the measured CO actually drops by about 5 ppbv. This again indicates that the measured EBC peak must be caused by a source that is rich in BC but poor in CO, consistent with the FLEXPART attribution to flaring. Thus, in this case we can attribute the measured EBC concentrations almost exclusively to gas flaring emissions in Russia.

On 27 February, the period with rather clean Arctic air arriving at Zeppelin ends, due to advection of air from Siberia until 3 March. During this pollution episode, the model simulates a mix of BC from flaring and other sources (including sources in Eastern Asia). The major flaring contribution in this case comes from the eastern region of intense flaring seen in Fig. 1. The model underestimates the measured EBC concentrations substantially, especially at the beginning of the episode. Remarkably, the flaring contribution is largest during the first part of the episode (27–28 February), which may suggest that especially flaring emissions have been underestimated. CO mixing ratios peak at a later time than the measured EBC, which is consistent with a shift from sources like flaring with a high average BC / CO emission ratio during the measured EBC peak to other sources (and probably also stronger removal) at later times.

3.3.3 Shipboard measurements downwind of the flaring region

FLEXPART backward simulations were initialized for the aerosol samples collected on board of the research vessel *Akademik Mstislav Keldysh*. While the EBC data has a temporal resolution of 10–14 h, ship position data were available only at the starting and ending time of each sample collection. Ten FLEXPART runs were initialized along an interpolated ship track during a sample collection period and their results were subsequently merged. The sparse ship position information introduces some uncertainty in the comparison of model results and measurements as the ship often moved by a few degrees of longitude and up to two degrees of latitude from one known position to the other. Also, we had no emission data for the year 2011 but used the 2010 emission data instead. For the comparison with the model results we excluded the first and the last measurement sample, which were collected in the harbor of Arkhangelsk, as well as one sample that was affected by on-board garbage burning. All three excluded samples had very high EBC concentrations.

From Arkhangelsk, the ship sailed to the northeast through the White, Barents and Kara Sea and back, passing directly north of the region with strong flaring emissions (for the ship track, see the top left panel of Fig. 6). Southeasterly winds

during the first few days of the campaign (when the ship was northwest of the flaring regions) and then southwesterly winds (when the ship was to the northeast of the flaring regions) delivered emissions from the flaring region to the ship until about 19–20 September. Indeed, flaring was the dominant source for the modeled BC concentrations, although residential combustion, agricultural biomass burning and other sources contributed as well. For days, the measured concentrations were more than one order of magnitude (and up to almost two orders of magnitude) higher than the September and October monthly average EBC concentrations measured at the Arctic research stations discussed earlier (compare with Fig. 8). Considering that the mass absorption efficiency assumed for converting the optical measurements to EBC was more than twice as high for the ship measurements than for the station measurements, the true difference in measured EBC mass concentrations may be even larger.

The model underestimates the measured concentrations almost continuously during this period as well as during the rest of the campaign (and would underestimate even more strongly when using a lower mass absorption efficiency). This suggests that our flaring emissions (and/or other BC emission sources) in this area are not over- but rather underestimated. The model does reproduce the measured strong decrease in EBC concentrations on 19 and especially on 21 September when the air started to come from the Arctic Ocean. From 24–25 September, the measured EBC concentrations increased again. This is in agreement with a change of advection pathway from the southeast. However, according to the simulations, the air was transported over land in areas without significant EBC emissions, so the modeled EBC concentrations remained low. This indicates that BC emissions also in areas east of the flaring regions, e.g., around Norilsk, may be underestimated. On 2 and 3 October, the air had again a mainly Arctic origin, explaining the drop in measured EBC concentrations. During the time of the measured EBC peak on 5–6 October, the air came again from the south and also included source areas on the Kola peninsula and Finland. The modeled retroplume just misses major source areas and was also influenced by strong wet scavenging. Thus, the model does not capture this peak.

Overall, the comparison between measured EBC and modeled BC concentrations for the ship campaign is poor. Most of the variations in the measurement data can be qualitatively explained by changing source areas of the sampled air masses, which confirms the validity of the measurements. Contamination by ship exhaust cannot be excluded totally for all samples but does not appear to be a critical problem. Possible reasons for the poor model performance are underestimated BC emissions and overestimated BC loss, or errors in the simulated transport. Since we do not consider the change of the hygroscopicity of the BC aerosol from hydrophobic to hydrophilic, an overestimation of loss processes close to the sources is expected. Therefore, we also calculated the BC concentrations for a passive tracer, where all BC emissions
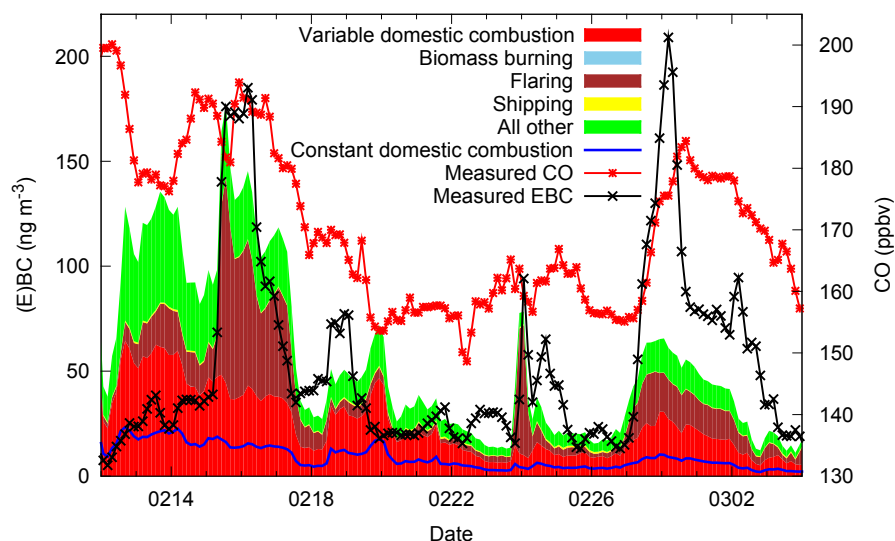
Fig. 9. Time series of measured EBC (black line with crosses) and carbon monoxide (red line with asterisks) as well as modeled BC split into different source categories (see color legend) for the Zeppelin station for the period 12 February until 4 March 2010. Also shown are the results for the residential combustion tracer with constant emission rate throughout the year (blue line).
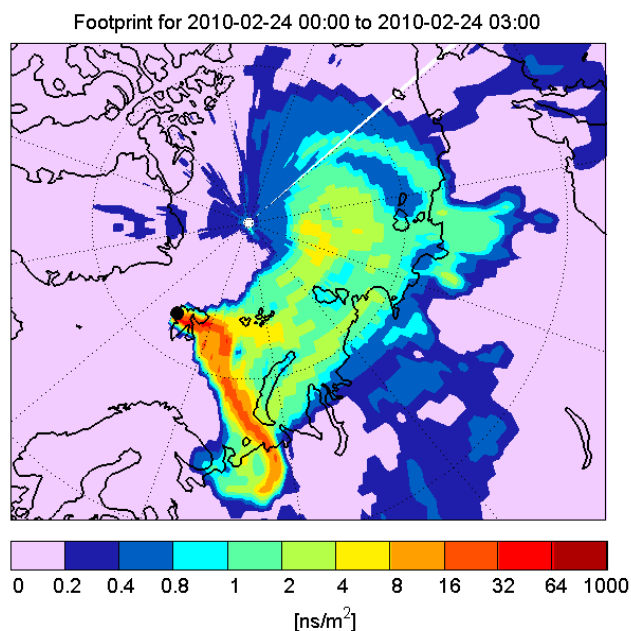

Fig. 10. Map of the footprint emission sensitivity of the BC aerosol tracer, for the air mass arriving at the Zeppelin station between 0 and 03:00 UTC on 24 February 2010. The Zeppelin station is marked with a black dot.

during the last 31 days before arrival of the air mass are accumulated without removal. In this case, the model roughly reproduces the observed concentration levels, and the relative contribution of flaring emissions is somewhat reduced (contributing about one third of the modeled BC). However, even

in this extreme scenario, the model does not systematically overestimate the measured concentrations. The general poor model performance is likely due to overall emission underestimates as well as due to erroneous spatial disaggregation. For instance, flaring emissions were attributed to rather large regions, as the positions of individual flares were not considered in the spatial emission disaggregation.

4   Discussion

4.1   Flaring emissions

The attribution of measured EBC to flaring emissions at Zeppelin is not always as clear as during the period discussed in Sect. 3.3.2 because long-range transport normally incorporates emissions from large source regions and a mixture of source types. However, there are many other episodes, for which the model-measurement comparison and the BC / CO enhancement ratios indicate large flaring contributions. In fact, using a statistical method, the flaring region in Russia was identified already by Hirdman et al. (2010) as the key source region for the highest measured EBC concentrations at Zeppelin, Barrow and Alert. However, Hirdman et al. (2010) could not attribute the EBC to flaring as a source type because at the time of their study information on flaring emissions was not available. Similarly, Eleftheriadis et al. (2009) for EBC (using a different instrument) and Tunved et al. (2013) for sub-micrometer aerosol mass concentration identified the same source region for the Zeppelin observatory. Earlier analyses also indicated a similar source region for EBC measured at Barrow and Alert (Sharma et al., 2006).
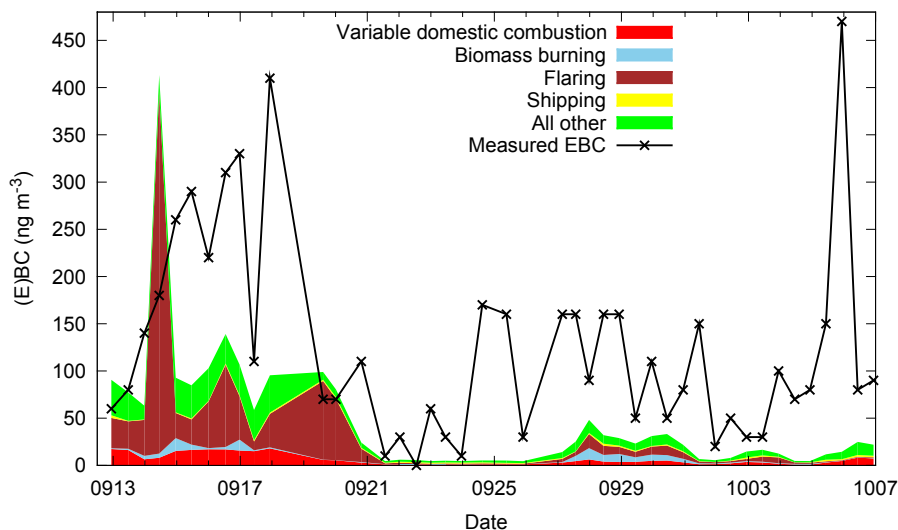
Fig. 11. Time series of measured EBC (black line with crosses) as well as modeled BC split into different source categories (see color legend) during the cruise of the research vessel *Akademik Mstislav Keldysh*.

While the flaring emissions are highly uncertain and accurate quantification of their contribution to Arctic BC will require more work, the case studies for Zeppelin suggest that it is unlikely that GAINS overestimates the emissions dramatically. Our comparison of these data to model calculations (Sect. 3.3.3) in fact suggests that the ECLIPSE emission estimates for the flaring region are too low. The poor skill of our model to reproduce the shipborne measurement data also indicates that the spatial distribution of the emissions is not accurate. This is expected since GAINS attributes the flaring emissions to two large regions and does not account for the spatial distribution of individual flares in these regions. Such emission disaggregation errors are critical for simulations of BC in proximity to the source regions (e.g., for simulating BC over the Kara Sea) but are probably less important further downwind (e.g., the Central Arctic). The model-measurement comparison in Sect. 3.3.3 also suggests that BC emissions further east in Siberia than the flaring regions are probably too low, which may indicate that GAINS underestimates BC emissions from other source types than flaring in Siberia as well.

Doherty et al. (2010) reported that the highest BC concentrations in snow for the entire Arctic were measured in northern Russia. Particularly high BC concentrations in snow were found near Vorkuta. Local contamination was suspected since the sampling was done only 30 km from the city (Doherty et al., 2010). However, we note that their sampling site was also only some 100 km away from the western area associated with gas flaring, which could be an alternative explanation for the high measured BC concentrations.

The BC emissions from gas flaring must also be seen in the context of on-going rapid changes in the petroleum industry not only in Russia but also in remote areas of North America and Europe. Associated gas in oil production is vented or flared in all regions where there is no infrastructure to store, utilize or transport the gas to consumers, which is typical for the oil production in remote areas. It is also predicted that petroleum activities will shift poleward (Peters et al., 2011), which raises concerns particularly for the Arctic.

4.2 Seasonality of the emissions

Regarding the seasonal cycle of residential combustion emissions, it is worth noticing that using daily resolved emissions does not only enhance surface concentrations of BC in the Arctic, but also reduces BC concentrations in the middle and lower latitudes. This could remedy the underestimates of BC in the Arctic that is common to most CTMs and CCMs and at the same time also help the models to avoid typical overestimates at lower latitudes (Bond et al., 2013). "Vertical transport that is too strong or scavenging rates that are too low" and "opposite biases in these processes" in the Arctic and elsewhere have been given as possible explanations for this (Bond et al., 2013). Our results suggest that the missing seasonality of residential combustion emissions as well as the lacking flaring emissions are also important.

While inclusion of daily variability enhances the modeled seasonal cycle of surface concentrations of BC in the Arctic, the measurements indicate that our modeled seasonality is still too weak. It is likely that seasonally varying efficiency of wet scavenging such as discussed in Browse et al. (2012) can largely explain this. However, it is also possible that missing seasonality of emissions from sectors other than residential combustion contributes to this. For instance, temporal (and spatial) distribution of emissions from non-road diesel engines and generators which are widely used in the Arctic, is

poorly characterized because of a lack of data. Such seasonality should be quantified and added to current emission data sets to further improve model simulations.

A consistent feature at all stations is that the measurements show higher concentrations in March–May than in October–December, whereas the model predicts relatively similar concentration levels for these periods. In addition to likely differences in wet scavenging efficiency, seasonality of the emissions not captured in our study could partly be responsible for this. For instance, energy demand for water heating is highest in spring when cold water inlet temperatures are substantially lower than in fall (Energy Saving Trust, 2008). Space heating requirements may also be slightly higher in spring than in fall for the same outside temperatures, due to the decrease of ground temperatures during winter. The corresponding shift of a fraction of the emissions from late fall to early spring would improve the modeled seasonality of Arctic BC concentrations. Another possibility are emissions from shipping. High-latitude shipping emissions are currently not well represented in global inventories both with respect to spatial as well as temporal distribution. Eckhardt et al. (2013) have shown that local emissions from cruise ships have an influence on the EBC measurements at Zeppelin from June to August. However, some ships already visit earlier in the year and this may also influence the seasonal cycle of EBC at least at Zeppelin.

4.3 The influence of aerosol removal on BC seasonality and flaring contribution

The emphasis of this paper was on the importance of seasonality in high-latitude emissions and on flaring as an emission source missing from current inventories. This does not mean that seasonality of BC ageing and wet scavenging are not important. Other studies (Liu et al., 2011; Huang et al., 2010a, b; Browse et al., 2012; Sharma et al., 2013) have shown that the seasonality of Arctic BC concentrations is also shaped by seasonally varying BC ageing and wet scavenging. Our model partly accounts for this seasonality; however, it ignores BC ageing and uses constant wet scavenging coefficients for all types of precipitation. Thus, seasonality in wet scavenging in our model is only due to seasonality in precipitation and in the relative location of clouds and BC. To illustrate to what extent seasonality in the aerosol removal affects our modeled BC concentrations, we compare our simulated BC concentrations with the BC concentrations obtained when assuming fixed BC lifetimes of 3 days and 10 days, respectively. In the annual mean, absolute concentrations are lowest for the 3-day tracer and highest for the 10-day tracer, with the aerosol tracer in between but close to the 10-day tracer. The left panel of Fig. 12 shows the results for the Zeppelin station (results for other stations are similar). In order to focus on the seasonality rather than on absolute concentration values, the simulated concentrations are normalized by their January values. The seasonality of simulated concentra-

tions for the 3-day tracer is much stronger than the seasonality for the 10-day tracer: BC concentrations in June are 2.9 % (7.5 %) of the January concentrations for the 3-day (10-day) lifetime tracer. This is expected because the slower transport into the Arctic in summer reduces the concentrations of short-lived species relatively more than those of longer-lived species compared to the winter situation (Stohl, 2006). Thus, for short-lived species a large part of the aerosol seasonality in the Arctic is simply due to seasonally varying transport efficiency. For wet scavenging operating with constant efficiency throughout the year, the seasonality of the aerosol tracer would fall between the seasonalities of the two fixed lifetime tracers. However, this is not the case. The aerosol tracer has a smaller seasonality even than the 10-day lifetime tracer, with the June concentrations being 9.8 % of the January concentrations. The seasonality is also "delayed", leading to relatively higher concentrations during late winter and spring than would be expected for a fixed-lifetime tracer with the same average lifetime. This shows that FLEXPART, at least qualitatively, captures an important aspect of Arctic haze, namely the relative inefficiency of aerosol removal in late winter and spring, compared to summer. This brings the shape of the simulated seasonal cycle closer to the observed BC cycle than for the fixed-lifetime tracers.

Notice, however, that in our model the reduced aerosol removal in winter and spring is only due to less precipitation. In reality, also the wet scavenging mechanisms are different (e.g., ice clouds vs. liquid water clouds) and different scavenging coefficients should be used to account for these differences. This is discussed in detail in Browse et al. (2012). Accounting for these differences would likely further improve the simulated seasonality. Similar arguments hold for slower BC ageing in winter, which reduces the scavenging efficiency as well. Nevertheless, as this paper has shown, the seasonal variability in the emissions is also important. Indeed, Sand et al. (2013) recently reported an improved performance of BC simulations in the Arctic with the new ECLIPSE emission data set also for an Earth system model.

The right panel of Fig. 12 shows the relative contribution of flaring emissions to total simulated BC from all sources at Zeppelin, for the three different tracers. The relative contribution throughout the year is largest for the shortest-lived tracer. This is a consequence of the high latitude location of the major flaring regions. For the Arctic, sources at high latitudes are more important than sources of equal strength at lower latitudes, and the relative difference of this importance increases with decreasing tracer lifetime. Similarly, the importance of accounting for daily emission variability at high latitudes increases with decreasing tracer lifetime (not shown). The lifetime of the BC aerosol tracer in our model is nearly 10 days, which is longer than the reported BC lifetime in most CTMs and CCMs. Consequently, the relative contribution of the flaring emissions simulated with these models would probably be larger than reported in this paper, and the importance of accounting for daily emission variability
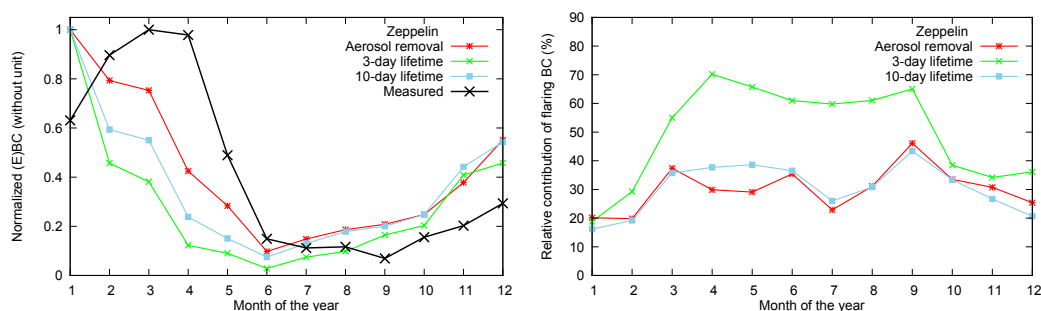
Fig. 12. The seasonal cycle of simulated BC concentrations at the Zeppelin station for the BC tracer with dry and wet aerosol removal, the BC tracer with a fixed 3-day lifetime, and the BC tracer with a fixed 10-day lifetime (left panel). For better comparison of seasonality, the simulated concentrations are normalized with the simulated January concentrations (62.8, 22.1, 107.4 ng m^{-3}, respectively, for the three tracers). Also shown are the measured EBC concentrations, normalized by the March concentration (56.7 ng m^{-3}). The right panel shows the relative contribution of flaring emissions to the total simulated concentration from all sources, for the three tracers.

would also be larger. Given the relatively long BC lifetime (due mainly to relatively inefficient wet scavenging) used in our model, our findings should be conservative. In reality, flaring emissions and daily emission variability may be even more important factors for explaining Arctic BC.

Finally, while the model simulations presented in this paper were done only for BC, the main results of this study should hold for other short-lived pollutant aerosols and gases as well. Both residential combustion as well as gas flaring are important sources also of other short-lived pollutants (e.g., organic carbon, nitrogen oxides, etc.).

5 Conclusions

BC emissions from gas flaring are less than 3 % of global BC emissions in the ECLIPSE emission data set but they dominate the BC emissions in the Arctic (latitudes greater than 66° N). Using these emissions for simulations with the Lagrangian particle dispersion model FLEXPART, we find that the flaring emissions contribute 42 % to the annual mean BC surface concentrations in the Arctic. Their contribution is largest in March when they account for 52 % of all Arctic BC near the surface. Most of the flaring BC in the Arctic resides close to the surface, so that the contribution of flaring emissions in the middle and upper troposphere is small.

We have derived a daily data set for residential combustion emissions, based on the heating degree day (HDD) concept. Using this data set and annually constant emissions, we found that in January the Arctic-mean surface concentrations of BC are 150 % higher when using daily emissions than when using annually constant emissions. Since concentration reductions in summer are smaller than the increases in winter, there is a systematic increase of Arctic-mean annual mean BC surface concentrations by 68 % when using daily emissions compared to annually constant emissions. A large

part (93 %) of this systematic increase can be captured also when using monthly emissions.

In a comparison with EBC measurements at six Arctic stations, we find that using daily varying residential combustion emissions and adding emissions from gas flaring substantially improves the simulated Arctic BC concentrations, both with respect to simulated concentration levels and seasonality as well as regarding the differences between the different stations.

Emissions from flaring normally arrive at the Arctic measurement stations mixed with emissions from other sources. This makes direct attribution of measured EBC to flaring difficult. For individual episodes, however, we could show that flaring emissions in Russia strongly influence EBC measurements at Zeppelin. During periods when flaring emissions arrive at Zeppelin, measured EBC typically increases strongly, while there is little impact on CO, which is consistent with an expected high BC / CO emission ratio of gas flaring.

Shipborne measurements during a cruise in the White, Barents and Kara seas north of the flaring region recorded EBC concentrations that are one to two orders of magnitude higher than those typically measured in the Arctic further away from Eurasia. The model could not reproduce these high concentrations, which suggests that EBC emissions in this area are still underestimated, even in our inventory which accounts for gas flaring.

A better quantification of gas flaring emissions of BC and other substances is urgently needed. Furthermore, targeted aerosol and atmospheric composition measurements at different distances to the gas flares need to be made, since the measurements used here are all too far away to allow studying air masses polluted by gas flares alone and/or allow no partitioning of the measured EBC into different source categories.

References

Amann, M., Bertok, I., Borken-Kleefeld, J., Cofala, J., Heyes, C., Höglund-Isaksson, L., Klimont, Z., Nguyen, B., Posch, M., Rafaj, P., Sander, R., Schöpp, W., Wagner, F., and Winiwarter, W.: Cost-effective control of air quality and greenhouse gases in Europe: modeling and policy applications, Environ. Mod. Software, 26, 1489–1501, doi:10.1016/j.envsoft.2011.07.012, 2011.

Barrie, L. A.: Arctic air pollution – an overview of current knowledge, Atmos. Environ., 20, 643–663, 1986.

Boman, C., Pettersson, E., Westerholm, R., Boström, D., and Nordin, A.: Stove performance and emission characteristics in residential wood log and pellet combustion, part 1: pellet stoves, Energy Fuels, 25, 307–314, doi:10.1021/ef100774x, 2011.

Bond, T. C. and Bergstrom, R. W.: Light absorption by carbonaceous particles: An investigative review, Aerosol Sci. Technol., 39, 1–41, 2005.

Bond, T. C., Streets, D. G., Yarber, K. F., Nelson, S. M., Woo, J. H., and Klimont, Z.: A technology-based global inventory of black and organic carbon emissions from combustion, J. Geophys. Res., 109, 1–43, doi:10.1029/2003JD003697, 2004.

Bond, T. C., Doherty, S. J., Fahey, D. W., Forster, P. M., Berntsen, T., DeAngelo, B. J., Flanner, M. G., Ghan, S., Kärcher, B., Koch, D., Kinne, S., Kondo, Y., Quinn, P. K., Sarofim, M. C., Schultz, M. G., Schulz, M., Venkataraman, C., Zhang, H., Zhang, S., Bellouin, N., Guttikunda, S. K., Hopke, P. K., Jacobson, M. Z., Kaiser, J. W., Klimont, Z., Lohmann, U., Schwarz, J. P., Shindell, D., Storelvmo, T., Warren, S. G., and Zender, C. S.: Bounding the role of black carbon in the climate system: A scientific assessment, J. Geophys. Res., 118, 5380–5552, doi:10.1002/jgrd.50171, 2013.

Bourgeois, Q. and Bey, I.: Pollution transport efficiency toward the Arctic: Sensitivity to aerosol scavenging and source regions, J. Geophys. Res., 116, D08213, doi:10.1029/2010JD015096, 2011.

Browse, J., Carslaw, K. S., Arnold, S. R., Pringle, K., and Boucher, O.: The scavenging processes controlling the seasonal cycle in Arctic sulphate and black carbon aerosol, Atmos. Chem. Phys., 12, 6775–6798, doi:10.5194/acp-12-6775-2012, 2012.

Cao, G., Zhang, X., and Zheng, F.: Inventory of black carbon and organic carbon emissions from China, Atmos. Environ., 40, 6516–6527, 2006.

CAPP: A recommended approach to completing the national pollutant release inventory (NPRI) for the upstream oil and gas industry, Canadian Association of Petroleum Producers (CAPP), available from: http://www.capp.ca/library/publications/policyRegulatory/pages/pubInfo.aspx?DocId=119572 (last access 19 March 2013), 2007.

Chen, Y., Zhi, G., Feng, Y., Liu, D., Zhang, G., Li, J., Sheng, G., and Fu, J.: Measurements of black and organic carbon emission factors for household coal combustion in China: implication for emission reduction, Environ. Sci. Technol., 43, 9495–9500, doi:10.1021/es9021766, 2009.

Corbett, J. J., Lack, D. A., Winebrake, J. J., Harder, S., Silberman, J. A., and Gold, M.: Arctic shipping emissions inventories and future scenarios, Atmos. Chem. Phys., 10, 9689–9704, doi:10.5194/acp-10-9689-2010, 2010.

Doherty, S. J., Warren, S. G., Grenfell, T. C., Clarke, A. D., and Brandt, R. E.: Light-absorbing impurities in Arctic snow, Atmos. Chem. Phys., 10, 11647–11680, doi:10.5194/acp-10-11647-2010, 2010.

Eckhardt, S., Hermansen, O., Grythe, H., Fiebig, M., Stebel, K., Cassiani, M., Baecklund, A., and Stohl, A.: The influence of cruise ship emissions on air pollution in Svalbard – a harbinger of a more polluted Arctic?, Atmos. Chem. Phys., 13, 8401–8409, doi:10.5194/acp-13-8401-2013, 2013.

EEA: EMEP/EEA air pollutant emission inventory guidebook, Technical report, European Environmental Agency (EEA), Copenhagen, Denmark, available from: http://www.eea.europa.eu/publications/emep-eea-emission-inventory-guidebook-2009 (last access 19 March 2013), 2009.

Eleftheriadis, K., Vratolis, S., and Nyeki, S.: Aerosol black carbon in the European Arctic: Measurements at Zeppelin station, Ny-Ålesund, Svalbard from 1998–2007, Geophys. Res. Lett., 36, L02809, doi:10.1029/2008GL035741, 2009.

Elvidge, C. D., Baugh, K. E., Tuttle, B. T., Howard, A. T., Pack, D. W., Milesi, C., and Erwin, E. H.: A twelve year record of national and global gas flaring volumes estimated using satellite data: final report to the World Bank, NOAA National Geophysical Data Center, Boulder, US, available from: http://www.ngdc.noaa.gov/dmsp/interest/gas_flares.html, 2007.

Elvidge Ch. D., Ziskin, D., Baugh, K. E., Tuttle, B. T., Ghosh, T., Pack, D. W., Erwin, E. H., and Zhizhin, M.: A fifteen year record of global natural gas flaring derived from satellite data, Energies, 2, 595–622, doi:10.3390/en20300595, 2009.

Elvidge, C. D., Baugh, K. E., Anderson, S., Ghosh, T., and Ziskin, D.: Estimation of gas flaring volumes using NASA MODIS fire detection products, NOAA National Geophysical Data Center, Boulder, US, available from: http://www.ngdc.noaa.gov/dmsp/interest/gas_flares.html (last access on 19 March 2013), 2011.

Energy Saving Trust: Measurement of domestic hot water consumption in dwellings, 62 pp., report available from: http://www.energysavingtrust.org.uk/Publications2/Housing-professionals/Monitoring/Measurement-of-domestic-hot-water-consumption-in-dwellings (last access: March 2013), 2008.

Flanner, M. G., Zender, C. S., Randerson, J. T., and Rasch, P. J.: Present-day climate forcing and response from black carbon in snow, J. Geophys. Res., 112, D11202, doi:10.1029/2006JD008003, 2007.

Garrett, T. J., Zhao, C., and Novelli, P.: Assessing the relative contributions of transport efficiency and scavenging to seasonal variability in Arctic aerosol, Tellus, 62B, 190–196, doi:10.1111/j.1600-0889.2010.00453.x, 2010.

Garrett, T. J., Brattström, S., Sharma, S., Worthy, D. E. J., and Novelli, P.: The role of scavenging in the seasonal transport of black carbon and sulfate to the Arctic, Geophys. Res. Lett., 38, L16805, doi:10.1029/2011GL048221, 2011.

Habib, G., Venkataraman, C., Bond, T. C., and Schauer, J. J.: Chemical, microphysical and optical properties of primary particles from the combustion of biomass fuels, Environ. Sci. Technol., 42, 8829–8834, doi:10.1021/es800943f, 2008.

Hansen, A. D. A., Rosen, H., and Novakov, T.: The aethalometer – an instrument for the real-time measurement of optical absorption by aerosol particles, Sci. Total. Environ., 36, 191–196, 1984.

Hertel, O., Christensen, J. Runge, E. H., Asman, W. A. H., Berkowicz, R., Hovmand, M. F., and Hov, O.: Development and testing of a new variable scale air pollution model – ACDEP, Atmos. Environ., 29, 1267–1290, 1995.

Hienola, A. I., Pietikäinen, J.-P., Jacob, D., Pozdun, R., Petäjä, T., Hyvärinen, A.-P., Sogacheva, L., Kerminen, V.-M., Kulmala, M., and Laaksonen, A.: Black carbon concentration and deposition estimations in Finland by the regional aerosol-climate model REMO-HAM, Atmos. Chem. Phys., 13, 4033–4055, doi:10.5194/acp-13-4033-2013, 2013.

Hirdman, D., Sodemann, H., Eckhardt, S., Burkhart, J. F., Jefferson, A., Mefford, T., Quinn, P. K., Sharma, S., Ström, J., and Stohl, A.: Source identification of short-lived air pollutants in the Arctic using statistical analysis of measurement data and particle dispersion model output, Atmos. Chem. Phys., 10, 669–693, doi:10.5194/acp-10-669-2010, 2010.

Huang, L., Gong, S. L., Jia, C. Q., and Lavoué, D.: Relative contributions of anthropogenic emissions to black carbon aerosol in the Arctic, J. Geophys. Res., 115, D19208, doi:10.1029/2009JD013592, 2010a.

Huang, L., Gong, S. L., Jia, C. Q., and Lavoué, D.: Importance of deposition processes in simulating the seasonality of the Arctic black carbon aerosol, J. Geophys. Res., 115, D17207, doi:10.1029/2009JD013478, 2010b.

Hyvärinen, A.-P., Kolmonen, P., Kerminen, V.-M., Virkkula, A., Leskinen, A., Komppula, M., Hatakka, J., Burkhart, J., Stohl, A., Aalto, P., Kulmala, M., Lehtinen, K. E. J., Viisanen, Y., and Lihavainen, H.: Aerosol black carbon at five background measurement sites over Finland, a gateway to the Arctic, Atmos. Environ. 45, 4042–4050, 2011.

IEA (International Energy Agency): World Energy Outlook 2011, International Energy Agency, Paris, France, 2011.

Johnson, M. R., Devillers, R. W., and Thomson, K. A.: Quantitative field measurement of soot emission from a large gas flare using Sky-LOSA, Environ. Sci. Technol., 45, 345–350, 2011.

Klimont, Z., Cofala, J., Xing, J., Wei, W., Zhang, C., Wang, S., Kejun, J., Bhandari, P., Mathur, R., Purohit, P., Rafaj, P., Chambers, A., Amann, M., and Hao, J.: Projections of SO_2, NO_x, and carbonaceous aerosols emissions in Asia, Tellus, 61B, 602–617, doi:10.1111/j.1600-0889.2009.00428.x, 2009.

Klimont, Z., Kupiainen, K., Heyes, Ch., Purohit, P., Cofala, J., Rafaj, P., and Schoepp, W.: Global anthropogenic emissions of particulate matter, in preparation, 2013.

Klonecki, A., Hess, P., Emmons, L., Smith, L., Orlando, J., and Blake, D.: Seasonal changes in the transport of pollutants into the Arctic troposphere – model study, J. Geophys. Res., 108, 8367, doi:10.1029/2002JD002199, 2003.

Koch, D., Schulz, M., Kinne, S., McNaughton, C., Spackman, J. R., Balkanski, Y., Bauer, S., Berntsen, T., Bond, T. C., Boucher, O., Chin, M., Clarke, A., De Luca, N., Dentener, F., Diehl, T., Dubovik, O., Easter, R., Fahey, D. W., Feichter, J., Fillmore, D., Freitag, S., Ghan, S., Ginoux, P., Gong, S., Horowitz, L., Iversen, T., Kirkevåg, A., Klimont, Z., Kondo, Y., Krol, M., Liu, X., Miller, R., Montanaro, V., Moteki, N., Myhre, G., Penner, J. E., Perlwitz, J., Pitari, G., Reddy, S., Sahu, L., Sakamoto, H., Schuster, G., Schwarz, J. P., Seland, Ø., Stier, P., Takegawa, N., Takemura, T., Textor, C., van Aardenne, J. A., and Zhao, Y.: Evaluation of black carbon estimations in global aerosol models, Atmos. Chem. Phys., 9, 9001–9026, doi:10.5194/acp-9-9001-2009, 2009.

Kristiansen, N. I., Stohl, A., and Wotawa, G.: Atmospheric removal times of the aerosol-bound radionuclides ^{137}Cs and ^{131}I measured after the Fukushima Dai-ichi nuclear accident – a constraint for air quality and climate models, Atmos. Chem. Phys., 12, 10759–10769, doi:10.5194/acp-12-10759-2012, 2012.

Kupiainen, K. and Klimont, Z.: Primary emissions of fine carbonaceous particles in Europe, Atmos. Environ., 41, 2156–2170, doi:10.1016/j.atmosenv.2006.10.066, 2007.

Lack, D., Lerner, B., Granier, C., Baynard, T., Lovejoy, E., Massoli, P., Ravishankara, A., and Williams, E.: Light absorbing carbon emissions from commercial shipping, Geophys. Res. Lett., 35, L13815, doi:10.1029/2008GL033906, 2008.

Law, K. S. and Stohl, A.: Arctic air pollution: Origins and impacts, Science, 315, 1537–1540, doi:10.1126/science.1137695, 2007.

Li, X. H., Wang, S. X., Duan, L., Hao, J. M., and Nie, Y. F.: Carbonaceous aerosol emissions from household biofuel combustion in China, Environ. Sci. Technol., 43, 6076–6081, 2009.

Liu, J., Fan, S., Horowitz, L. W., and Levy II, H.: Evaluation of factors controlling long-range transport of black carbon to the Arctic, J. Geophys. Res., 116, D04307, doi:10.1029/2010JD015145, 2011.

Liu, X., Easter, R. C., Ghan, S. J., Zaveri, R., Rasch, P., Shi, X., Lamarque, J.-F., Gettelman, A., Morrison, H., Vitt, F., Conley, A., Park, S., Neale, R., Hannay, C., Ekman, A. M. L., Hess, P., Mahowald, N., Collins, W., Iacono, M. J., Bretherton, C. S., Flanner, M. G., and Mitchell, D.: Toward a minimal representation of aerosols in climate models: description and evaluation in the Community Atmosphere Model CAM5, Geosci. Model Dev., 5, 709–739, doi:10.5194/gmd-5-709-2012, 2012.

Lu, Z., Zhang, Q., and Streets, D. G.: Sulfur dioxide and primary carbonaceous aerosol emissions in China and India, 1996–2010, Atmos. Chem. Phys., 11, 9839–9864, doi:10.5194/acp-11-9839-2011, 2011.

Lund, M. T. and Berntsen, T.: Parameterization of black carbon aging in the OsloCTM2 and implications for regional transport to the Arctic, Atmos. Chem. Phys., 12, 6999–7014, doi:10.5194/acp-12-6999-2012, 2012.

McEwen, J. D. N. and Johnson, M. R.: Black carbon particulate matter emission factors for buoyancy driven associated gas flares, J. Air Waste Manag. Assoc., 63, 307–321, doi:10.1080/10473289.2011.650040, 2012.

McMahon, T. A. and Denison, P. J.: Empirical atmospheric deposition parameters – a survey, Atmos. Environ., 13, 571–585, 1979.

Meinander, O., Kazadzis, S., Arola, A., Riihelä, A., Räisänen, P., Kivi, R., Kontu, A., Kouznetsov, R., Sofiev, M., Svensson, J., Suokanerva, H., Aaltonen, V., Manninen, T., Roujean, J.-L., and Hautecoeur, O.: Spectral albedo of seasonal snow during intensive melt period at Sodankylä, beyond the Arctic Circle, Atmos. Chem. Phys., 13, 3793–3810, doi:10.5194/acp-13-3793-2013, 2013.

Nguyen, Q. T., Skov, H., Sørensen, L. L., Jensen, B. J., Grube, A. G., Massling, A., Glasius, M., and Nøjgaard, J. K.: Source apportionment of particles at Station Nord, North East Greenland during 2008–2010 using COPREM and PMF analysis, Atmos. Chem. Phys., 13, 35–49, doi:10.5194/acp-13-35-2013, 2013.

Parashar, D. C., Gadi, R., Mandal, T. K., and Mitra, A. P.: Carbonaceous aerosol emissions from India, Atmos. Environ., 39, 7861–7871, 2005.

Peters, G. P., Nilssen, T. B., Lindholt, L., Eide, M. S., Glomsrød, S., Eide, L. I., and Fuglestvedt, J. S.: Future emissions from shipping and petroleum activities in the Arctic, Atmos. Chem. Phys., 11, 5305–5320, doi:10.5194/acp-11-5305-2011, 2011.

Pettersson, E., Boman, C., Westerholm, R., Boströom, D., and Nordin, A.: Stove performance and emission characteristics in residential wood log and pellet combustion, part 2: wood stove, Energy Fuels, 25, 315–323, doi:10.1021/ef1007787, 2011.

Plejdrup, M. S., Nielsen, O.-K., and Nielsen, M.: Emission inventory for fugitive emissions in Denmark, Technical report, National Environmental Research Institute (NERI), Aarhus, Denmark, available from: http://www.dmu.dk/Pub/FR739.pdf (last access 19 March 2013), 2009.

Quayle, R. G. and Diaz, H. F.: Heating degree day data applied to residential heating energy consumption, J. Appl. Meteor., 19, 241–246, 1980.

Quinn, P. K., Bates, T. S., Baum, E., Doubleday, N., Fiore, A. M., Flanner, M., Fridlind, A., Garrett, T. J., Koch, D., Menon, S., Shindell, D., Stohl, A., and Warren, S. G.: Short-lived pollutants in the Arctic: their climate impact and possible mitigation strategies, Atmos. Chem. Phys., 8, 1723–1735, doi:10.5194/acp-8-1723-2008, 2008.

Quinn, P. K., Stohl, A. Arneth, A., Berntsen, T., Burkhart, J. F., Christensen, J., Flanner, M., Kupiainen, K., Lihavainen, H., Shepherd, M., Shevchenko, V., Skov, H., and Vestreng, V.: The Impact of Black Carbon on Arctic Climate. Arctic Monitoring and Assessment Programme (AMAP), Oslo, 72 pp., ISBN-978-82-7971-069-1, 2011.

Sand, M., Berntsen, T. K., Seland, Ø., and Kristjansson, J. E.: Arctic surface temperature change to emissions of black carbon within Arctic or midlatitudes, J. Geophys. Res., 118, 7788–7798, doi:10.1002/jgrd.50613, 2013.

Schmidl, C., Luisser, M., Padouvas, E., Lasselsberger, L., Rzaca, M., Cruz, C. .-S., Handler, M., Peng, G., Bauer, H., and Puxbaum, H.: Particulate and gaseous emissions from manually and automatically fired small scale combustion systems, Atmos. Environ., 45, 7443–7454, 2011.

Sharma, S., Andrews, E., Barrie, L. A., Ogren, J. A., and Lavoue, D.: Variations and sources of the equivalent black carbon in the high Arctic revealed by long-term observations at Alert and Barrow: 1989–2003, J. Geophys. Res., 111, D14208, doi:10.1029/2005JD006581, 2006.

Sharma S., Ishizawa, M., Chan, D., Lavoué, D., Andrews, E., Eleftheriadis, K., and Maksyutov, S.: 16-year simulation of Arctic black carbon: Transport, source contribution, and sensitivity analysis on deposition, J. Geophys. Res. Atmos., 118, 943–964, doi:10.1029/2012JD017774, 2013.

Shaw, G. E.: The Arctic Haze phenomenon, B. Am. Meteorol. Soc., 76, 2403–2412, 1995.

Shindell, D. T., Chin, M., Dentener, F., Doherty, R. M., Faluvegi, G., Fiore, A. M., Hess, P., Koch, D. M., MacKenzie, I. A., Sanderson, M. G., Schultz, M. G., Schulz, M., Stevenson, D. S., Teich, H., Textor, C., Wild, O., Bergmann, D. J., Bey, I., Bian, H., Cuvelier, C., Duncan, B. N., Folberth, G., Horowitz, L. W., Jonson, J., Kaminski, J. W., Marmer, E., Park, R., Pringle, K. J., Schroeder, S., Szopa, S., Takemura, T., Zeng, G., Keating, T. J., and Zuber, A.: A multi-model assessment of pollution transport to the Arctic, Atmos. Chem. Phys., 8, 5353–5372, doi:10.5194/acp-8-5353-2008, 2008.

Slinn, W. G. N.: Predictions for particle deposition to vegetative canopies, Atmos. Environ., 16, 1785–1794, 1982.

Stohl, A.: Characteristics of atmospheric transport into the Arctic troposphere, J. Geophys. Res., 111, D11306, doi:10.1029/2005JD006888, 2006.

Stohl, A. and Thomson, D. J.: A density correction for Lagrangian particle dispersion models, Bound.-Lay. Meteor., 90, 155–167, 1999.

Stohl, A., Hittenberger, M., and Wotawa, G.: Validation of the Lagrangian particle dispersion model FLEXPART against large scale tracer experiment data, Atmos. Environ., 32, 4245–4264, 1998.

Stohl, A., Forster, C., Eckhardt, S., Spichtinger, N., Huntrieser, H., Heland, J., Schlager, H., Wilhelm, S., Arnold, F., and Cooper, O.: A backward modeling study of intercontinental pollution transport using aircraft measurements, J. Geophys. Res., 108, 4370, doi:10.1029/2002JD002862, 2003.

Stohl, A., Forster, C., Frank, A., Seibert, P., and Wotawa, G.: Technical note: The Lagrangian particle dispersion model FLEXPART version 6.2, Atmos. Chem. Phys., 5, 2461–2474, doi:10.5194/acp-5-2461-2005, 2005.

Stohl, A., Andrews, E., Burkhart, J. F., Forster, C., Herber, A., Hoch, S. W., Kowal, D., Lunder, C., Mefford, T., Ogren, J. A., Sharma, S., Spichtinger, N., Stebel, K., Stone, R., Ström, J., Tørseth, K., Wehrli, C., and Yttri, K. E.: Pan-Arctic enhancements of light absorbing aerosol concentrations due to North American boreal forest fires during summer 2004, J. Geophys. Res., 111, D22214, doi:10.1029/2006JD007216, 2006.

Textor, C., Schulz, M., Guibert, S., Kinne, S., Balkanski, Y., Bauer, S., Berntsen, T., Berglen, T., Boucher, O., Chin, M., Dentener, F., Diehl, T., Easter, R., Feichter, H., Fillmore, D., Ghan, S., Ginoux, P., Gong, S., Grini, A., Hendricks, J., Horowitz, L., Huang, P., Isaksen, I., Iversen, I., Kloster, S., Koch, D., Kirkevåg, A., Kristjansson, J. E., Krol, M., Lauer, A., Lamarque, J. F., Liu, X., Montanaro, V., Myhre, G., Penner, J., Pitari, G., Reddy, S., Seland, Ø., Stier, P., Takemura, T., and Tie, X.: Analysis and quantification of the diversities of aerosol life cycles within AeroCom, Atmos. Chem. Phys., 6, 1777–1813, doi:10.5194/acp-6-1777-2006, 2006.

Tissari, J., Sippula, O., Kouki, J., Vuorio, K., and Jokiniemi, J.: Fine particle and gas emissions from the combustion of agricultural fuels fired in a 20 kW burner, Energy Fuels, 22, 2033–2042,

doi:10.1021/ef700766y, 2008.

Tissari, J., Hytonen, K., Sippula, O., and Jokiniemi, J.: The effects of operating conditions on emissions from masonry heaters and sauna stoves, Biomass and Bioenergy, 33, 513–520, 2009.

Tunved, P., Ström, J., and Krejci, R.: Arctic aerosol life cycle: linking aerosol size distributions observed between 2000 and 2010 with air mass transport and precipitation at Zeppelin station, Ny-Ålesund, Svalbard, Atmos. Chem. Phys., 13, 3643–3660, doi:10.5194/acp-13-3643-2013, 2013.

US EPA: Compilation of air pollutant emission factors - volume I: stationary point and area sources, AP-42 5th Edition, US Environmental Protection Agency (US EPA), Springfield, VA, 1995.

van der Werf, G. R., Randerson, J. T., Giglio, L., Collatz, G. J., Mu, M., Kasibhatla, P. S., Morton, D. C., DeFries, R. S., Jin, Y., and van Leeuwen, T. T.: Global fire emissions and the contribution of deforestation, savanna, forest, agricultural, and peat fires (1997–2009), Atmos. Chem. Phys., 10, 11707–11735, doi:10.5194/acp-10-11707-2010, 2010.

Van Vuuren, D. P., Edmonds, J. A., Kainuma, M., Riahi, K., Thomson, A. M., Hibbard, K., Hurtt, G. C., Kram, T., Krey, V., Lamarque, J.-F., Masui, T., Meinshausen, M., Nakicenovic, N., Smith, S. J., and Rose, S.: The representative concentration pathways: an overview, Climatic Change, 109, 5–31, 2011.

Venkataraman, C., Habib, G., Eiguren-Fernandez, A., Miguel, A. H., and Friedlander, S. K.: Residential biofuels in South Asia: carbonaceous aerosol emissions and climate impacts, Science, 307, 1454–1456, 2005.

Vignati, E., Karl, M., Krol, M., Wilson, J., Stier, P., and Cavalli, F.: Sources of uncertainties in modelling black carbon at the global scale, Atmos. Chem. Phys., 10, 2595–2611, doi:10.5194/acp-10-2595-2010, 2010.

WMO (World Meteorological Organization): Guidelines for the Measurement of Atmospheric Carbon Monoxide, GAW Report No. 192, World Meteorological Organization, Geneva, Switzerland, 2010.

Zhang, Q., Streets, D. G., Carmichael, G. R., He, K. B., Huo, H., Kannari, A., Klimont, Z., Park, I. S., Reddy, S., Fu, J. S., Chen, D., Duan, L., Lei, Y., Wang, L. T., and Yao, Z. L.: Asian emissions in 2006 for the NASA INTEX-B mission, Atmos. Chem. Phys., 9, 5131–5153, doi:10.5194/acp-9-5131-2009, 2009.

Zhi, G., Chen, Y., Feng, Y., Xiong, S., Li, J., Zhang, G., Sheng, G., and Fu, J.: Emission characteristics of carbonaceous particles from various residential coal-stoves in China, Environ. Sci. Technol., 42, 3310–3315, doi:10.1021/es702247q, 2008.

Zhi, G., Peng, C., Chen, Y., Liu, D., Sheng, G., and Fu, J.: Deployment of coal briquettes and improved stoves: possibly an option for both environment and climate, Environ. Sci. Technol., 43, 5586–5591, doi:10.1021/es802955d, 2009.